[AMERICAN JOURNAL OF SCIENCE, VOL. 282, MARCH, 1982, P. 193-236]

American Journal of Science

March 1982

DISSOLUTION OF CALCITE IN THE DEEP-SEA: THEORETICAL PREDICTION FOR THE CASE OF UNIFORM SIZE PARTICLES SETTLING INTO A WELL-MIXED SEDIMENT

ROBIN S. KEIR*

Department of Geology and Geophysics, Yale University, New Haven, Connecticut 06520

ABSTRACT. A model for the dissolution of calcareous sediment has been formulated with the following assumptions: (1) that the particles are well-stirred on the time scale of their dissolution, (2) that the reactive surface area is proportional to the number concentration of the carbonate particles, (3) that the dissolution kinetics are a non-linear function of the undersaturation of the pore water, and (4) that the dissolution is forced by the undersaturation of the overlying water column.

Using titration alkalinity and total CO_2 analysis from the GEOSECS expedition, various estimates of the undersaturation with respect to calcite versus water depth can be made. Using this input, the model can reproduce the observed percent $CaCO_3$ versus depth curves for various regions of the Atlantic and Pacific Oceans. However, the rate constant necessary to do this is sensitive to the scale of undersaturation. The use of Mehrbach and others (1974) as opposed to Lyman's (ms) second apparent dissociation for carbonic acid for the calculation of K_{sp}' results in a rate constant two orders of magnitude larger.

The model will *not* satisfactorily predict the foraminiferal dissolution index curve observed by Berger (1975) because of the assumption that the particles are well mixed in the zone of dissolution. The implication is that the solution susceptible forams dissolve in less than half a year after entering the abyss. The observed percent $CaCO_3$ versus depth curve in this area suggests that the *minimum* time of dissolution of the *most resistant* carbonate fraction is from 0.5 yr (from Mehrbach and others constants) to 6 yrs (from Lyman's constants). Thus, it appears that the fine fraction is as resistant or more resistant to dissolution compared to solution susceptible forams.

By making an *ad hoc* assumption that when 15 percent of the susceptible forams remain in the sediment, they are no longer recognizable as of a particular species, the provisional estimate can be made that 10 to 30 percent of the settling calcite dissolves at the R_0 level and 50 to 65 percent dissolves at the inflection point of the foraminiferal lysocline in the central and western equatorial Pacific Ocean.

* Present address: Geological Research Division, Scripps Institution of Oceanography, La Jolla, California 92093

INTRODUCTION

The veneer of sediment at the interface with seawater in the abyss of the oceans acts as a chemical reactor in which calcium carbonate dissolves. Recently, it has been recognized that the nature of this reactor is determined by the dissolution kinetics of the various carbonate particles in contact with the overlying seawater and the interstitial water and by those physical factors that affect mixing and transport of both the solid sediment particles and the dissolved carbonate ion in the pore water (Takahashi and Broecker, 1977; Schink and Guinasso, 1977).

The understanding of how this "reactor" behaves is of particular interest in light of the following:

1. Most of the calcium carbonate falling from the surface layer appears to reach the bottom intact, without undergoing appreciable dissolution (Berger and Piper, 1972; Adelseck and Berger, 1975; Honjo, 1975, 1977). Thus, the processes affecting dissolution at the sediment-water interface play a major role in controlling the regeneration of alkalinity into the water column and in controlling the carbonate content (percent $CaCO_3$) and carbonate faunal assemblages in deep-sea sediment.

2. Based on the sediment record of percent calcium carbonate, facies distributions, ratio of fragments to whole tests of forams, and oxygen isotope ratios, it appears that deep-sea sediments have undergone substantial dissolution cycles during the upper Pleistocene (for example, Arrhenius, 1952; Broecker, 1971; Berger, 1973; Gardner, 1975; Luz and Shackleton, 1975; Berger, 1977).

3. Over the next one or two centuries, mankind will inject a substantial pulse of CO_2 into the atmosphere, part of which will eventually find its way into the deep-sea and react with the carbonate sediment. Whether trying to unravel the past or predict the future, it is essential that one understands how the processes involved at the sediment-water interface influence dissolution and how the sediment responds to environmental changes such as a change in the undersaturation of the overlying water (Broecker and Takahashi, 1977).

It was discovered during the earliest oceanographic expeditions that the mass fraction of calcium carbonate in deep-sea sediment generally decreased with increasing depth. In addition, the character of the carbonate sediment changes. Spinose, fragile species of foraminifera disappear with increasing depth. This was quantized into a foram dissolution index by Berger (1968, 1975). The average grain size of sediment diminishes with depth which is likely associated with the fragmentation of forams because of dissolution (Johnson, Hamilton, and Berger, 1977). There also appears to be less diversity of the nannofossils with increasing depth (Roth and Berger, 1975). All these features are associated with the increasing dissolution rate of carbonate sediment.

In this paper, I shall attempt to explain the character of partially dissolved sediment by the interaction of ionic diffusion in the sediment interstitial water, bioturbation, sedimentation rate, the dissolution kinet-

ics of calcite, and the degree of undersaturation of the overlying water. It is assumed that the influx of solid to the interface occurs by sedimentation and that this influx is uniform with regions considered. Although this is a gross oversimplification, it will prove instructive with regard to the predicted sedimentological features.

The characteristics, which will be addressed, are the relationship of percent $CaCO_3$ to water depth in various areas of the Atlantic and Pacific Oceans, the foraminiferal dissolution index as a function of depth in the equatorial Pacific, and the state of saturation with respect to calcite in these areas. This is similar to the approach of Takahashi and Broecker (1977), Schink and Guinasso (1977), and Emerson and Bender (1981), but this model contains two unique features: (1) the rate kinetics are formulated as a power law which is observed in experimental laboratory studies, and (2) the surface area available for dissolution is formulated proportional to the number of carbonate particles.

First, a simple model, which assumes all settling particles are of uniform shape, will be considered. Then, the model will be slightly elaborated to include two types of settling carbonate particles, each with its own size and reactivity. This model will be used as an analog to a faunal assemblage change as a function of depth.

Both models are simplifications of the actual situation. Other factors may exert various influences on the dissolution and observed accumulation. These are oxidation of organic matter at the interface and within the pore water, continuous redeposition of fine-grain material downslope, and laminar boundary layers overlying the interface. There is not yet any way of quantitatively evaluating these three factors except in the last case by the use of engineering models (Schink and Guinasso, 1977). Nevertheless, the simple model serves to give some insight on the actual situation.

A. ONE TYPE OF CARBONATE PARTICLE

1. Theory

The assumptions of the model are as follows:

1. that the carbonate particles impinging on the sediment are homogeneous in size and shape and that these particles dissolve at a uniform rate, for any constant degree of undersaturation of the surrounding seawater, until they disappear. Such would be the ideal case of disks or thin shells of uniform thickness dissolving uniformly over their surfaces;

2. that the particles are well-stirred to a depth greater than the depth over which significant dissolution takes place;

3. that the concentration of carbonate ion in the pore water is controlled exclusively by molecular diffusion and dissolution of calcium carbonate;

4. that the reactive surface area of the solid carbonate is proportional to the number of carbonate particles (regardless of the amount of dissolution any individual particle has undergone) and that the dissolution rate is a power function of the undersaturation as defined below; and

5. that the system is at steady state, that is the input, standing crop, and dissolution flux of carbonate are invariant in time.

The first assumption is a very crude approximation which, although it is not correct insofar as what deep-sea sediment is observed to consist of, serves as a vehicle greatly to simplify the mathematical formulation of the model, and it also serves to give insight into the behavior of an idealized system which may not behave all that differently from the "real world."

The second assumption is reasonable with the possible exception of the sediments near the CCD where particles may be destroyed on a time scale shorter than the rate they are mixed downward by bioturbation. There are two considerations. First, from the distribution of Pb^{210} in deep-sea sediment, it appears sediment is mixed in the upper 8 cm or so on a much shorter time scale than the time scale of advection due to burial (Nozaki and others, 1977; Peng, Broecker, and Berger, 1979).

Second, the solid will appear to be well-mixed unless the time for removal via dissolution of the particles is shorter than the time scale of mixing. The latter is approximately given by X_1^2/D_B where X_1 is the depth to which dissolution occurs in the sediment and D_B is the apparent "diffusion" coefficient of sediment due to bioturbation. As will be shown later (sec. 6c), virtually all dissolution is confined to the upper 3 mm in highly dissolved, carbonate poor sediments. From the average D_B of Pb^{210} profiles on deep-sea sediment (Nozaki and others, 1977) of about 0.15 cm^2/yr, we obtain a mixing time on the order of half a year. Also, in this situation the minimum time of removal of a particle due to dissolution is predicted to be about 1 to 6 yrs, so the assumption of a well-mixed system appears self-consistent even in heavily dissolved sediments. However, as will be shown in part B, this assumption does not appear to be supported by the field evidence, at least in the case of the solution susceptible forams at depths greater than the bottom of the foraminiferal lysocline.

Figure 1 illustrates schematically the nature of the model. Calcite and insoluble solid particles enter at the upper boundary of a hypothetical box, the upper boundary representing the sediment-water interface. After entering the sediment, the particles are mixed to a depth, L, below the interface by bioturbation. Although the solid is mixed slowly compared to molecular diffiusion in the interstitial water, the mixing of particles is rapid compared to their rate of burial and alteration by dissolution, and therefore they will appear well-mixed in the sediment mixing zone. When significant dissolution occurs, the interstitial water saturates very rapidly with depth below the interface, and the dissolution is confined to a thin veneer of surface sediment.

The problem is, for a given flux of carbonate and insoluble material into the sediment and a given undersaturation of the overlying seawater, to calculate the fraction of the settling carbonate that dissolves and the

carbonate content and relative concentration of carbonate particles in the accumulating sediment.

It is assumed that the sedimentation of carbonate and insoluble material within a particular geographic region is the same, and therefore the sediment accumulated in relatively shallow locations where the overlying seawater is saturated is indicative of the influx of material reaching a deeper location where dissolution is occurring. The flux of total *solid volume* which leaves the box, that is, accumulates, at depth L at any particular location is

$$\frac{\psi_c}{\rho_c} + \frac{\psi_I}{\rho_I} = \omega(1-\phi) \ , \qquad (1)$$

where ψ_c and ψ_I refer to the mass flux of carbonate and insoluble material leaving the box at x = L, ρ_c and ρ_I refer to the density of the calcite and insoluble material, ϕ is the porosity, and ω the accumulation rate. In the case of no dissolution, we write eq (1) with the notation

$$\frac{\psi_c^\circ}{\rho_c} + \frac{\psi_c^\circ}{\rho_I} = \omega_o(1-\phi_o) \quad \text{(no dissolution)} \qquad (1A)$$

where ω_o and ϕ_o are the observed accumulation rate and porosity in the undissolved sediment.

With the assumption that the sediment influx of carbonate and insoluble material is the same at both locations, the flux of dissolved carbonate out of the sediment, J, is given by the difference in the mass

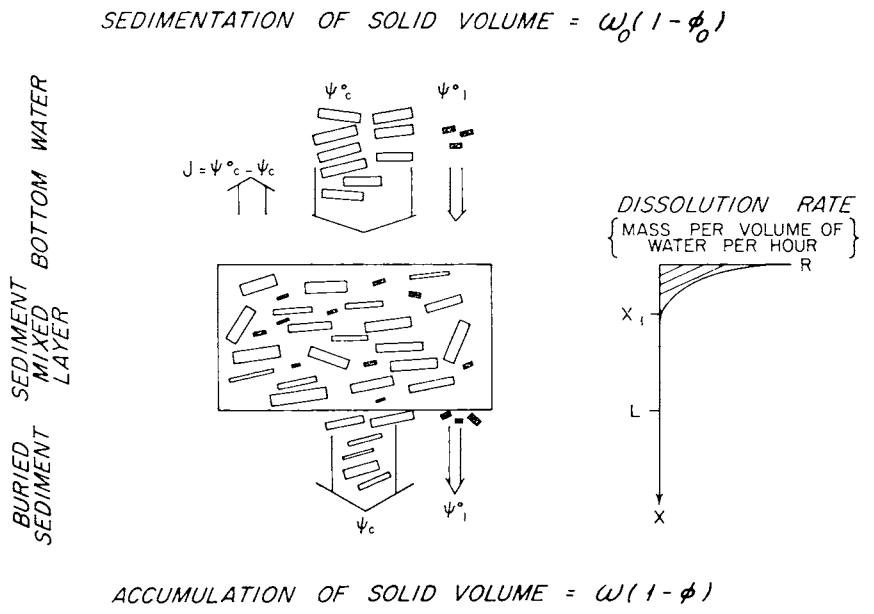

Fig. 1. Schematic of the model. Difference in accumulation of solid volume is $\omega_o(1-\phi_o) - \omega(1-\phi)$, which is due to removal of carbonate influx (ψc^o) by dissolution.

accumulation rate of the carbonate. Since $\psi_I = \psi_I^\circ$, we obtain from eqns (1) and (1A),

$$J = \psi_c^\circ - \psi_c = \rho_c[\omega_o(1-\phi_o) - \omega(1-\phi)] \tag{2}$$

The accumulation rate when dissolution occurs is given by

$$\omega = \frac{1}{1-\phi}\left[\omega_o(1-\phi_o) - \frac{J}{\rho}\right], \tag{3}$$

from here on where $\rho = \rho_c$ refers to the calcite density. We will make one more simplification which is that the porosity is invariant, that is, $\phi = \phi_o$ in which case

$$\omega = \omega_o - \frac{J}{\rho(1-\phi)} \tag{4}$$

This assumption is not strictly true. Arrhenius (1952) has shown that $(1-\phi)$ tends to increase by about a factor of two from carbonate-rich to carbonate-poor sediments. Nevertheless, this assumption simplifies the mathematical complexity of the problem, and so it will be adopted here.

When dissolution is occurring, two mechanisms remove solid carbonate particles from the sediment "mixed-layer" as follows: (1) the particles may be lost due to the net accumulation of sediment burying them below the mixed-layer, or (2) the carbonate particles may be completely dissolved before leaving the mixed-layer. For a given accumulation rate, ω, the characteristic time for the first mechanism is the contact time,

$$\tau = L/\omega$$

It is the time that it takes for the sediment to accumulate one mixed-layer upward. The reciprocal, $1/\tau$, is the frequency with which one mixed-layer thickness accumulates. τ also represents the average residence time of an insoluble particle in the mixed-layer. In the case of the carbonate particles, dissolution also can remove them from the mixed-layer in which case the residence time of these particles is shorter than τ.

We formulate the frequency of mxied-layer accumulation by dividing eq (4) by the length of the box, L, such that

$$\frac{1}{\tau} = \frac{1}{\tau_o} - \frac{J}{L\rho(1-\phi)} \tag{5}$$

where $\tau_o = L/\omega_o$ is the average contact time of particles in the box if no dissolution occurs.

In the model, it is assumed that *the surface area available for dissolution is proportional to the concentration of carbonate particles in the box*. To solve simultaneously for both the particle concentration and J, it is necessary to solve two equations, the steady state equation for the particle concentration and the steady state equation for the balance between diffusion and production of carbonate ions in the pore water.

Since the rate of change of particle concentration, β, is zero,

$$\frac{d\beta}{dt} - \frac{\beta_o}{\tau_o} = \frac{\beta}{\tau} - P = 0 \qquad \text{(steady state)} \tag{6}$$

The first term on the right is the input rate of particles per unit volume to the box. β_o is the concentration of particles (in particles per total volume), which would be in the box if no dissolution occurred. The second term is the output rate of particles due to burial. β is the particle concentration in the box. P is the rate of removal of particles per unit bulk volume due to dissolution and is a function of sedimentation rate and degree of undersaturation of the overlying seawater. P is not directly analogous to the dissolution flux, because it is the rate of complete destruction of the particles in the mixed-layer. Part of the dissolution flux is contributed by particles that only partially dissolve before burial.

We shall formulate P in terms of a characteristic time, t_p, that the carbonate particle takes to dissolve. It is assumed that particles of a uniform size enter the box, and if the dissolution were uniform over the entire mixed-layer, t_p would be a constant for all particles. However, in this model the dissolution is localized near the interface (upper) boundary to the box. If the mixing of particles were infinitely rapid throughout the box, again t_p would be a constant for all particles, because each particle would spend exactly the same amount of time in the dissolution zone as any other particle that entered the box at the same time. The development of the model will follow this point of view. However, while it has been shown that sediment mixing in the dissolution zone is rapid compared to dissolution of the particles, mixing does not occur infinitely rapidly throughout the entire sediment mixed-layer below the dissolution zone (about 8 cm in length). Thus, some particles that dissolve completely may spend most of the time near the interface, and others may spend a good deal of time below the dissolution zone, the latter particles having longer dissolution times than the former. However, the contact time, τ, also increases with the length of mixed-layer. It will be shown below that the ratio, t_p/τ, is independent of the thickness of the mixed-layer. Because we assume a steady-state system, the distribution of particles at various stages of dissolution (that is, with different thicknesses) which are below the zone where dissolution takes place is identical to that distribution mixed into and out of the zone itself. As the particles *in* the zone of dissolution are mixed rapidly compared to their dissolution, the entire mixed-layer will appear well-mixed, and despite the fact that t_p will vary from particle to particle, t_p/τ will be invariant.

It can be shown that the fraction of particles that have been added to the box at a given instant, $t = 0$, which would remain in the box at a later time, t, is $e^{-t/\tau}$ (Denbigh, 1944). For example, if a labeled concentration of particles, β_o^*, is added to the box at $t = 0$, the concentration remaining at time t is

$$\beta^* = \beta_o^* e^{-t/\tau} \tag{7}$$

Obviously, those particles that have not escaped from the box by burial before their time of complete dissolution has elapsed will no longer exist. Assuming for the moment that we have infinitely rapid mixing and that t_p is the same for all particles, it can be seen from eq (7) that the fraction

of incoming particles removed by dissolution is $e^{-t_p/\tau}$. Since P is the input rate times the fractional removal by dissolution we obtain

$$P = \frac{\beta_o}{\tau_o} e^{-t_p/\tau} \tag{8}$$

Substitution of eq (8) into (6) yields

$$\frac{\beta_o}{\tau_o}\left(1 - e^{-t_p/\tau}\right) - \frac{\beta}{\tau} = 0 \tag{9}$$

To obtain the characteristic time for total dissolution of a particle, t_p, first note that the rate of loss of solid per unit bulk volume due to dissolution is J/L. Because it has been assumed that all carbonate particles lose mass at the same rate and that the particle concentration is uniform in the box, the dissolution rate per particle is $J/(\beta L)$, which at steady state is constant. Dividing this quantity into the original mass per particle, σ_o, yields the characteristic time for the particle to completely dissolve, that is,

$$t_p = \frac{\beta \sigma_o L}{J} \tag{10}$$

However, from the undissolved box, we observe that

$$\beta_o \sigma_o = X_o \rho_s (1 - \phi) \tag{11}$$

where X_o is the mass fraction of calcium carbonate in the undissolved assemblage, and ρ_s is the average density of the solid. Since $\rho_s \cong \rho$, we obtain from eqs (10) and (11)

$$t_p = \frac{\beta}{\beta_o} \frac{X_o \rho (1 - \phi) L}{J} \tag{12}$$

Multiplying eq (12) by (5) yields

$$\begin{aligned} \frac{t_p}{\tau} &= \frac{\beta}{\beta_o} X_o \left[\frac{\rho(1-\phi)L}{J\tau_o} - 1\right] \\ &= \frac{\beta}{\beta_o} X_o \left[\frac{\rho(1-\phi)\omega_o}{J} - 1\right] \\ &= \frac{\beta}{\beta_o} X_o \left(F^{-1} - 1\right) \end{aligned} \tag{13}$$

Here F is defined as the ratio of the dissolution flux, J, to the total flux entering the box,

$$F = \frac{J}{\rho(1-\phi)\omega_o}$$

It is important to note that the result in eq (13) shows that the time ratio t_p/τ is independent of L, the size of the box. Thus, it is only necessary that the particles be mixed well in the zone where dissolution takes place, which in general is smaller than L.

By substitution of eqs (5) and (13) into (9) and multiplying by τ_o/β_o we obtain

$$1 - \frac{\beta}{\beta_o}(1-F) - \exp\left[- \frac{\beta}{\beta_o} X_o (F^{-1} - 1) \right] = 0 \qquad (14)$$

In this fashion, one obtains the steady state equation describing the ratio of the concentration of particles in the box relative to the case of no dissolution. To solve it, F must be formulated as a function of β/β_o and the solution chemistry. This is accomplished by assuming that at steady state, production of carbonate ions in the pore water by dissolution is balanced by ionic diffusion across the sediment water interface. Thus,

$$D' \frac{d^2c}{dx^2} + \frac{R}{M} = 0 \ , \qquad (15)$$

where c is the concentration and D′ the apparent diffusion coefficient of carbonate ion in the pore water, R is the rate of carbonate ion production in mass per volume of pore water, and M is the formula weight of $CaCO_3$ —100 mg/mmole.[1]

Experimental studies of the dissolution kinetics of calcite show that the rate of dissolution in mass dissolved per mass of solid carbonate per unit time, Q, is given by (Morse, 1978; Keir, 1980)

$$Q = k\, s^n \qquad (16A)$$

where s is the undersaturation factor defined as

$$s \equiv 1 - \frac{c}{c_{eq}} \ ,$$

and c_{eq} is the equilibrium dissolved carbonate ion concentration. The proportionality constant, k, is in the same units as Q. In this paper *the parameter, k, is restricted to undissolved sediment.* k is defined as the "rate constant," given in eq (16A), for the solid calcium carbonate particles in *undissolved* sediment. To obtain R, which is in units of mass per unit pore water volume per time, one must multiply Q by the mass of *undissolved* carbonate per unit pore water volume and by any change in reactive surface area between undissolved and partially dissolved sediment. The former quantity is given by $\beta_o\sigma_o/\phi$. Since it is assumed that

[1] The following points of clarification may be in order concerning the use of eq (15):

(A) Transport by burial advection of pore water is assumed to be negligible.

(B) Unlike the solid, the pore water cannot be treated as well-mixed. For example, using $D' = 10^{-6}$ cm^2s^{-1}, the mixing time is 25 hrs for a 0.3 cm length scale. However, the time scale of "pseudosaturation", that is, that time that the dissolution rate becomes negligible in a closed system is on the order of 30 min in this study (see also Broecker and Takahashi, 1978). Thus the pore water tends to saturate rapidly compared to mixing.

(C) Eq (15) ignores the reaction of dissolved $CO_3^=$ with other weak acids in solution, mainly boric acid. Because of the limited capacity of $H3BO_3$ to react, the rate constant in this study will only change by a factor of two (Keir, ms). As the rate constant is much more sensitive to uncertainty in the scale of undersaturation (sec. 3, and following), this is not a serious limitation in this study.

the reactive surface area is proportional to the carbonate particle concentration, β, the reactive surface area of partially dissolved relative to undissolved sediment is given by β/β_o.

Thus,

$$R = k\frac{\beta\sigma_o}{\phi} s^n \tag{16B}$$

Substituting eq (11) into (16B) one obtains

$$R = k\frac{X_o\rho(1-\phi)}{\phi}\frac{\beta}{\beta_o} s^n \tag{16C}$$

From the definition of s we see that

$$\frac{ds}{dx} = -\frac{1}{c_{eq}}\frac{dc}{dx}$$

Substitution of this relationship and eq (16C) into eq (15) yields

$$c_{eq}D'\frac{d^2s}{dx^2} - kX_o\frac{\beta}{\beta_o}\frac{\rho(1-\phi)}{\phi M} s^n = 0 ,$$

or

$$\frac{d^2s}{dx^2} - \gamma s^n = 0 , \tag{17}$$

where

$$\gamma \equiv \frac{kX_o\dfrac{\beta}{\beta_o}\rho(1-\phi)}{\phi M c_{eq}D'}$$

For the solution of (17), let $p = ds/dx$, and since

$$\frac{dp}{dx} = \frac{dp}{ds}\frac{ds}{dx} = p\frac{dp}{ds} ,$$

eq (17) becomes

$$p\frac{dp}{ds} - \gamma s^n = 0 \tag{18}$$

Separating the variables and integrating, we obtain

$$\frac{ds}{dx} = \pm\left(\frac{2\gamma}{n+1} s^{n+1} + C_1\right)^{1/2} , \tag{19}$$

where C_1 is the constant of integration. As will appear later (sec. 6D), virtually all the dissolution takes place in the box (except when there are miniscule degrees of undersaturation in the overlying water) so that

$$\int_0^L R\,dx \cong \int_0^\infty R\,dx.$$

As a good approximate solution, we note that as $x \to \infty$, $ds/dx \to 0$, and $s \to 0$; therefore $C_1 = 0$. The flux out of the sediment is (remember J is defined as positive, out of the box)

$$J = \phi M D' \frac{dc}{dx}\bigg|_{x=0}$$

$$= -\phi M D' c_{eq} \frac{ds}{dx}\bigg|_{x=0} \tag{20}$$

Substitution of the negative root in eq (19) into (20) yields

$$J = \phi D' M c_{eq} \left(\frac{2\gamma}{n+1} s_o^{n+1}\right)^{1/2}, \tag{21}$$

where s_o is the value of s at the sediment-water interface. We shall assume for the most part that s_o is equal to the undersaturation of the overlying bottom water, s_w. Schink and Guinasso (1977, 1978) have suggested that $s_o < s_w$ because of the presence of a laminar diffusive sublayer above the sediment-water interface. Transport of dissolved carbonate ion in this layer is limited to molecular diffusion. This results in reduction of the dissolution rate, because carbonate ion cannot be mixed rapidly into the overlying water. We will consider briefly the effect of a laminar boundary layer in section 5D.

From the definition of γ, we obtain

$$J = \left[\frac{2}{n+1}\rho(1-\phi)\phi D' c_{eq} M k X_o \frac{\beta}{\beta_o} s_o^{n+1}\right]^{1/2}, \tag{22}$$

and

$$\frac{J}{\rho(1-\phi)} = \left[\frac{2\phi D' c_{eq} M}{(n+1)\rho(1-\phi)} k X_o \frac{\beta}{\beta_o} s_o^{n+1}\right]^{1/2},$$

$$= \left[k X_o b(z) s_o^{n+1} \frac{\beta}{\beta_o}\right]^{1/2} \tag{23}$$

where

$$b(z) = \frac{2\phi D' M}{(n+1)\rho(1-\phi)} c_{eq} \tag{23a}$$

The term, b(z), increases with water depth, z, because the equilibrium concentration of carbonate ion, c_{eq}, increases with increasing pressure. To obtain F we divide eq (23) by ω_o,

$$F = \left[\frac{k}{\omega_o^2} X_o b(z) s_o^{n+1} \frac{\beta}{\beta_o}\right]^{1/2} \tag{24}$$

Thus we have the dissolution flux to total flux ratio formulated in the following terms: (1) two independent parameters, which are k/ω_o^2, the ratio of the rate constant to sedimentation rate squared, and X_o, the percent calcium carbonate of the settling assemblage, (2) a depth dependent constant, bs_o^{n+1}, and (3) the unknown surface area factor β/β_o which is also an index of the relative particle concentration.

For the purposes of calculation ϕ will be presumed constant with a value of 0.7. Johnson, Hamilton, and Berger (1977) show that Ontong-

Java Plateau sediments, with a range of 90 to 70 percent $CaCO_3$, are fairly constant with this value. With $D' = 60$ cm²/yr (Li and Gregory, 1974) and $n = 4.5$ (Keir, 1980), b has a value of

$$b = 1.87\, c_{eq} \frac{cm^2}{ky}$$

when c_{eq} is expressed in mmole/l.

Substitution of eq (24) into (14) yields the complete equation

$$1 - \frac{\beta}{\beta_o}\left[1 - \left(\frac{k}{\omega_o^2} X_o b s_o^{n+1} \frac{\beta}{\beta_o}\right)^{1/2}\right]$$
$$-\exp\left\{-\frac{\beta}{\beta_o} X_o \left[\left(\frac{k}{\omega_o^2} X_o b s_o^{n+1} \frac{\beta}{\beta_o}\right)^{-1/2} - 1\right]\right\} = 0 \qquad (25)$$

This transcendental function can be solved iteratively for β/β_o (details are provided elsewhere, Keir, ms). There are in general two solutions. The correct solution can be ascertained from the fact that J must be less than or equal to the influx of calcium carbonate due to sedimentation or in other words $F \leqslant X_o$. The spurious solution comes with $F > X_o$.

The ratio of outflux to dissolution to influx of carbonate due to sedimentation is

$$\frac{J}{J_{max}} = \frac{J}{X_o \omega_o \rho (1-\phi)} = \frac{F}{X_o} \qquad (26)$$

where $J_{max} = \psi_c{}^o$. From this ratio, the mass fraction of calcium carbonate, X, which is in the box and subsequently buried can be obtained from (Morse and Berner, 1972)

$$X = \frac{X_o\left(1 - \frac{J}{J_{max}}\right)}{1 - X_o \frac{J}{J_{max}}} = \frac{X_o - F}{1 - F} \qquad (27)$$

The profile of the concentration of dissolved carbonate ion versus depth can be obtained by integrating eq (19). With the condition that $s = s_o$ at $x = 0$, the result is

$$\left(\frac{s}{s_o}\right)^{\frac{n-1}{2}} = \left\{(n-1)\left[\frac{\gamma}{2(n+1)} s_o^{n-1}\right]^{1/2} x + 1\right\}^{-1} \qquad (28)$$

2. Percent $CaCO_3$ versus Water Depth in the Atlantic and Pacific Oceans

Recently, compilation of percent $CaCO_3$ in surficial sediment versus water depth was made on a regional basis for the Atlantic (Biscaye, Kolla, and Turekian, 1976), Pacific (Berger, Adelseck, and Meyer, 1976) and Indian Oceans (Kolla, Be, and Biscaye, 1976). For the purpose of testing this model, the Atlantic and Pacific data will be examined because GEOSECS profiles of titration alkalinity and total CO_2 permit calculation

of saturation factor profiles over large extents of these oceans. Adjacent subdivisions of the Atlantic and Pacific Oceans which appear to have similar profiles of percent $CaCO_3$ versus water depth were identified, and similarity was assessed by overlaying profiles of the various regions and judging qualitatively if two or more were similar. Although the scatter of the data in many cases prevents determining to what degree areas which appear similar are actually similar, distinct differences can be recognized between certain areas, and these can be mutually excluded. The results of this grouping are shown in figure 2.

3. Uncertainties in GEOSECS data and apparent thermodynamic constants used in calculation of s_w

The GEOSECS expedition provided worldwide analyses of titration alkalinity and total CO_2. In principle, s_w can be calculated from this data and plotted as a function of water depth for any particular station. Unfortunately, there is some uncertainty as to the accuracy of the data, despite the fact that on most legs, very precise results were obtained. In particular, it was recently suggested that the total CO_2 results in the Pacific Ocean are systematically high by about 0.015 mmole/kg, whereas those measured in the Atlantic were suggested to be correct on the basis of the agreement between calculated P_{CO_2} and oceanographic measurements (Takahashi and others, 1976; Broecker and Takahashi, 1978).

There are two other problems that obstruct unambiguous calculation of s_w. The apparent solubility product[2] of calcite in seawater, Ksp′, near 0°C and 1 atm pressure and the effect of pressure on Ksp′ are not agreed on (for example, see Edmond and Gieskes, 1970; Takahashi, 1975; Berner, 1976; Broecker and Takahashi, 1977). This leads to a disagreement of at

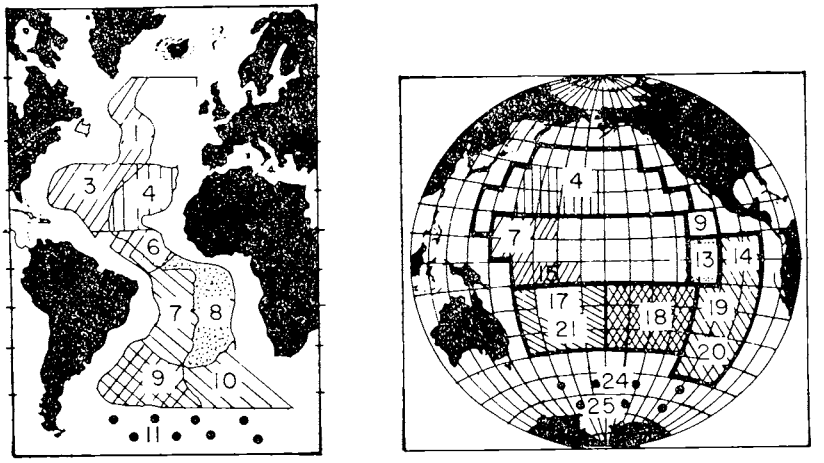

Fig. 2. Location of regions with similar percent $CaCO_3$ versus water depth (indicated by hatching) according to data in Biscaye, Kolla, and Turekian (1976) and Berger, Adelseckm and Neyer (1976). Index number shown is taken from the above publications.

least 0.2 in the calculated s_w. In addition, Mehrbach and others (1974) redetermined the apparent dissociation constants of carbonic acid in seawater and reported a K_2' value[3] about 14 percent lower than Lyman at 2°C. Because the laboratory determination of the equilibrium carbonate ion concentration, C_{eq}, is made using pH and titration alkalinity, use of Mehrbach and others' constants increases the saturation factor,

$$\Omega \cong \frac{c}{c_{eq}} .$$

This is because computation of the in-situ carbonate concentration, c, from total CO_2 and alkalinity is altered very little if Mehrbach and others rather than Lyman's constants are used (Takahashi and others, 1976), but the computed c_{eq} from pH and alkalinity is lowered about 14 percent. As a result, s_0 decreases by about 0.12.

All the above considerations prevent an unequivocal determination of the s_w versus ocean depth curves. The GEOSECS titration alkalinity and total CO_2 is currently under review, and although further corrections of the data are likely to be small (Brewer, personal commun.), final results are uncertain at present.

In this paper, model predicted percent $CaCO_3$ versus depth will be presented on the basis of s_w calculated from the following: (1) the most recently available GEOSECS titration alkalinity and total CO_2 except that the Pacific total CO_2 data set is not adjusted using the scheme of Broecker and Takahashi (1978), (2) same as (1) except that 0.015 mmole/kg is subtracted from the Pacific total CO_2 data, and (3) same as (2) except that the calculation of carbonate ion is made using the scheme of Broecker and Takahashi (1978). In (1) and (2) above, Lyman's (ms) apparent constants for the dissociation of carbonic acid in seawater were used. In (3), Mehrbach and others' (1974) constants were employed. In all cases, the pressure correction of Culberson and Pytkowicz (1968) to the apparent dissociation constants, the low temperature apparent solubility product measurement of Ingle and others (1973), and the apparent partial molal volume for dissolution of calcium carbonate suggests by Culberson (ms) based on Pytkowicz and Fowler (1967) were used. Both larger low temperature, 1 atm apparent solubility products (Hindman, ms; Berner, 1976) and larger pressure coefficients have been advocated (Ingle, 1975; Sayles, 1980). Model results based on this possibility are reported elsewhere (Keir, ms).

4. Calculation of s_w and percent $CaCO_3$ versus depth

s_w is calculated from titration alkalinity and total CO_2 by first calculating the in-situ carbonate ion concentration (Keir, 1979), and then

[2] $K_{sp}' = [Ca^{++}]\,[CO_3^{--}]$ at equilibrium with calcite.

[3] $K_2' = \frac{a_H\,[CO_3^{=}]}{[HCO_3^{-}]}$

Brackets refer to total ion concentration.
a_H is hydrogen ion activity.

estimating Ksp′ according to the method of Takahashi (1975). In the simplest case, it is assumed that $s_o = s_w$. From eqs (25), (26), and (27), percent $CaCO_3$ of the sediment versus s_o can be calculated for any assumed values of k/ω_o^2 and X_o. This is converted to a percent $CaCO_3$-versus-water depth plot via the s_o-versus-water depth curve calculated from the GEOSECS data. On a similar diagram, the observed percent $CaCO_3$ versus depth can be plotted. For various values of k/ω_o^2 and X_o, different model curves may be tested for correspondence with the actual data.

5. Percent $CaCO_3$ versus depth

A. *Based on Lyman's constants and "uncorrected" Pacific total CO_2 data.*—Three curves have been drawn in figure 3, A to D, in which the points represent data from the area shown in the inset. The curves are drawn for k/ω_o^2 which vary by a factor of three, thus the envelope represents an order of magnitude variation in k or a variation of a factor of three in sedimentation rate, ω_o. Many of the observed points lie close to the solid line, although large deviations occur, and in general there is considerable scatter in the data.

The curves in figure 3 have been found from trial and error and give a fair representation of the data. They are not best fit curves in any statistical sense. For those areas where large scatter in the data exists, the curve was chosen to represent the envelope of the data. Table 1 lists the values of $k/\omega_o^2$for the four solid curves in figure 3, A to D, and in addition also lists values of k/ω_o^2 found similarly in the other eight oceanic regions, which are illustrated elsewhere (Keir, ms).

TABLE 1

k/ω_o^2 for various regions of the Atlantic and Pacific Oceans

Area	k/ω_o^2 (ky/cm²) LU	MC	LC
Pacific 4	$1.1(10)^4$		
Atlantic 1-3-6	$2.1(10)^4$	$3(10)^6$	
Pacific 18	$8(10)^3$	$3(10)^6$	
Pacific 7-15	$2.1(10)^3$	$1.5(10)^5$	10^4
Atlantic 4	$6(10)^4$	$3(10)^6$	
Antarctic	$1.1(10)^4$		
Atlantic 9	$2.1(10)^4$		
Pacific 13	$1.8(10)^4$	10^7	$2(10)^5$
Atlantic 7-10	$8(10)^3$		
Pacific 17-21	$5.3(10)^3$		
Atlantic 8	$1.1(10)^4$		
Pacific 9-14-19-20	$8(10)^3$		

Laboratory measure

Sediment	$k(ky^{-1})$	k/ω_o^2*
Entire OJ sediment	$1.1(10)^7$	$0.8(10)^6$
> 300 μ OJ sediment	$2.1(10)^5$	$1.4(10)^4$

* Based on ω_o = 2.2 cm/ky and an Arrhenius activation energy of 8.4 kcal/mole.

s_o versus depth calculated using Lyman's constants and uncorrected ΣCO_2 in Pacific (LU), 'corrected' ΣCO_2 (LC), and Mehrbach and others' (1974) constants and 'corrected' Pacific ΣCO_2 (MC).

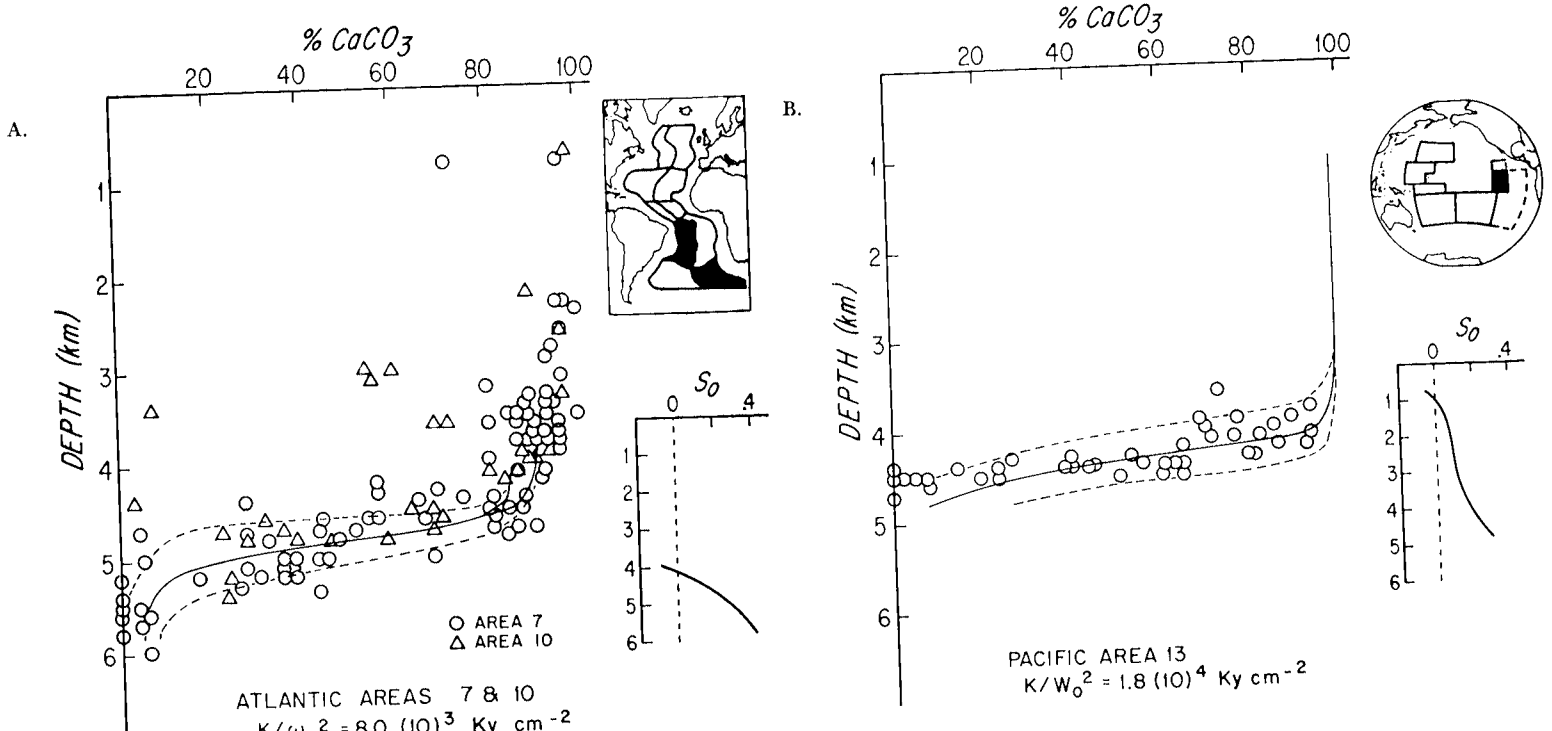
A.
% CaCO3
20
40
60
80
100
DEPTH (km)
1
2
3
4
5
6
So
0
4
AREA 7
AREA 10
ATLANTIC AREAS 7 & 10
K/ω0² = 8.0 (10)³ Ky cm⁻²
B.
% CaCO3
20
40
60
80
100
DEPTH (km)
So
0
4
PACIFIC AREA 13
K/W0² = 1.8 (10)⁴ Ky cm⁻²

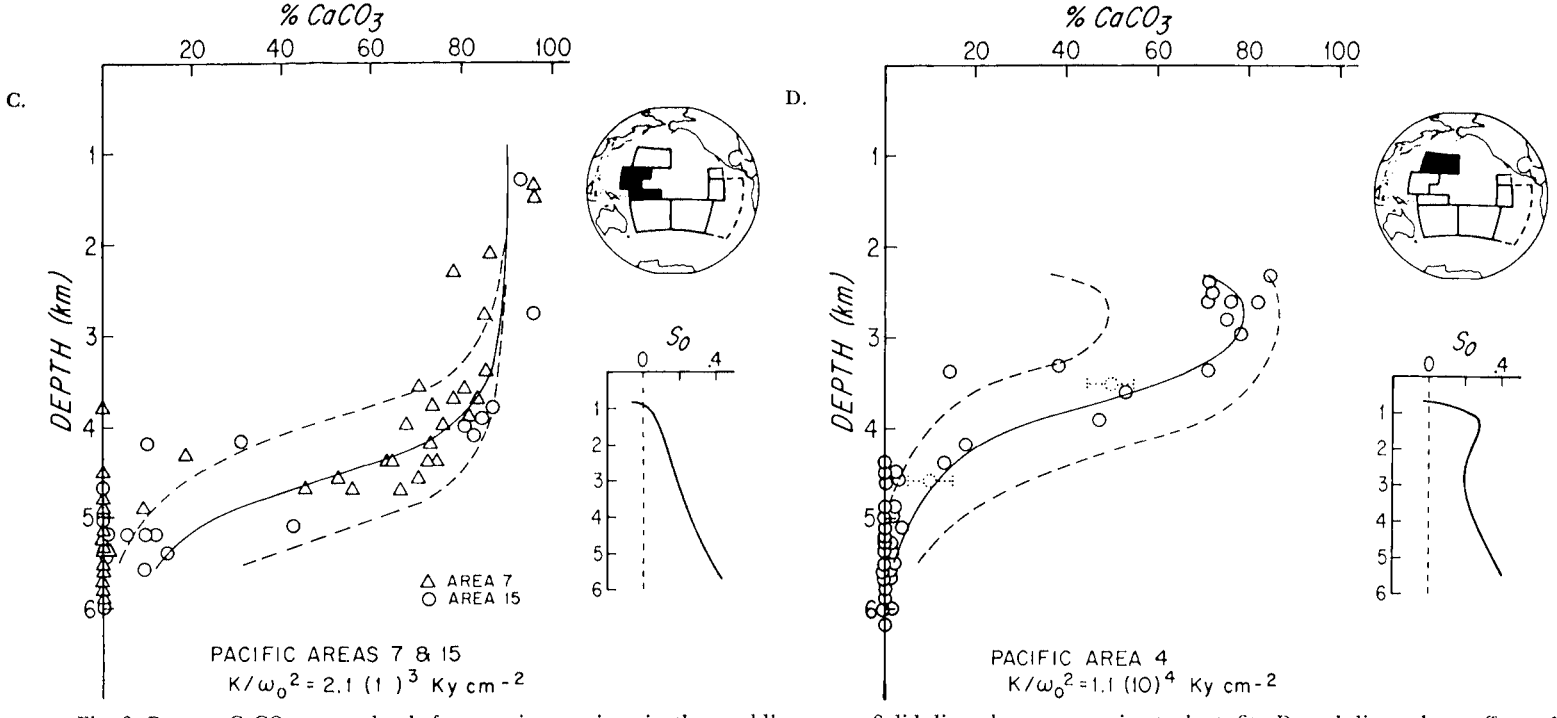

Fig. 3. Percent $CaCO_3$ versus depth from various regions in the world's oceans. Solid line shows approximate best fit. Dotted lines show effect of variation of k/ω_n^2 by a factor of three. Insets show area location and s_0 versus water depth calculated from GEOSECS A_t and ΣCO_2 using Lyman's (ms) K_1, K_2, and K_3 and Ingle and others (1973) calcite solubility value. Pacific total CO_2 data are not corrected. Data are from Biscaye, Kolla, and Turekian (1976) and Berger, Adelseck, and Meyer (1976).

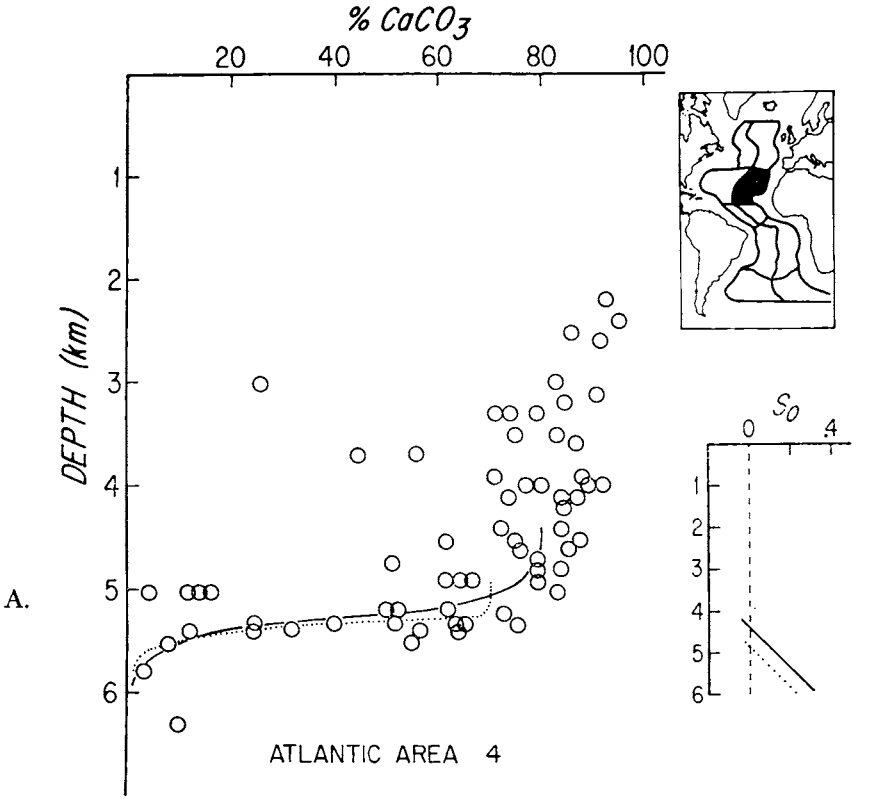
% CaCO3
20
40
60
80
100
DEPTH (km)
1
2
3
4
5
6
So
0
.4
ATLANTIC AREA 4

A.

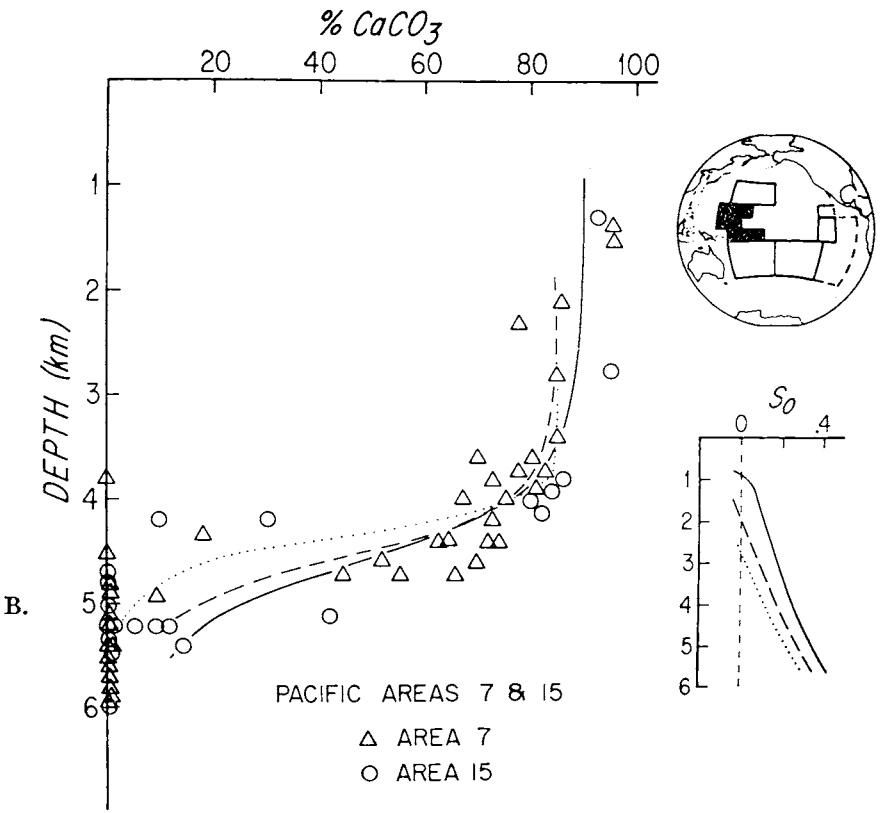
% CaCO3
20
40
60
80
100
DEPTH (km)
1
2
3
4
5
6
So
0
.4
PACIFIC AREAS 7 & 15
△ AREA 7
○ AREA 15

B.

B. *Comparison of predicted percent $CaCO_3$ versus depth based on three s_o computation schemes.*—Figure 4, A to C, compares the calculated percent $CaCO_3$ versus depth from the three (or two) s_o versus depth curves calculated according to the methods detailed in section 3. Each curve represents the best correspondence found by trial and error to the observed data. Other percent $CaCO_3$ versus depth profiles derived from the s_o versus depth scheme of Broecker and Takahashi (1978) can be found elsewhere (Keir, ms).

C. *Comparison of model derived and laboratory measured rate constants.*—Table 1 gives the approximate best value of k/ω_o^2 found by trial and error for each area from the three different s_o versus depth curves. If Lyman's constants are used to calculate s_o, the Atlantic k/ω_o^2 range from $8(10)^3$ to $6(10)^4$ ky cm^{-2}. If the "uncorrected" Pacific GEOSECS data are

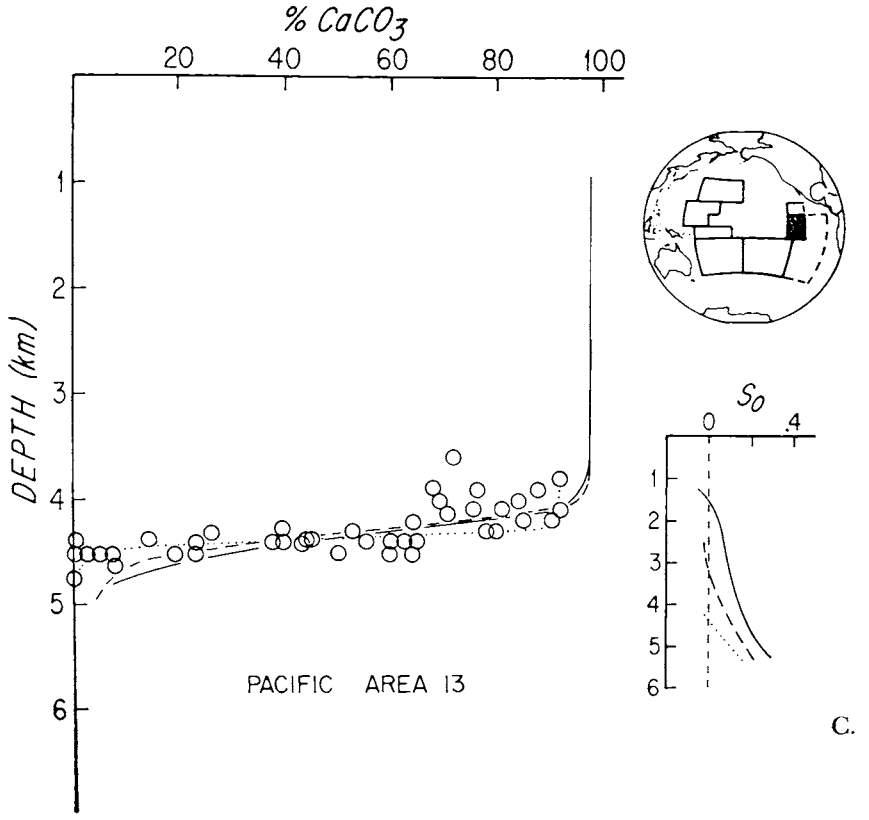

Fig. 4. Comparison of percent $CaCO_3$ versus depth obtained from three different undersaturation versus depth functions in the Pacific and two in the Atlantic. Solid line and dashed line show results based on Lyman's (ms) constants. Dashed line shows result when 0.015 μmole/kg is subtracted from Pacific GEOSECS total CO_2 data. Dotted line shows results based on Mehrbach and others (1974) constants (Broecker and Takahashi, 1978). Values of k/ω_o^2 in ky/cm^2 are as follows: (A) solid line $6(10)^4$, dotted line $3(10)^6$, (B) solid line $2.1(10)^3$, dashed line $(10)^4$, dotted line $1.5(10)^5$ and (C) solid line $1.8(10)^4$, dashed line $2(10)^5$, dotted line 10^7.

used the range is $2.1(10)^3$ to $1.8(10)^4$ ky cm^{-2}, whereas if the "corrected" Pacific data is used, k/ω_o^2 ranges from 10^4 to $2(10)^5$ ky cm^{-2}. If Mehrbach and others' constants and "corrected" Pacific data are employed, k/ω_o^2 is between $1.5(10)^5$ and 10^7 ky/cm^2. In all cases, the western equatorial Pacific yields k/ω_o^2 values about five to ten times lower than the rest of the Pacific. This may be due to a larger carbonate sedimentation rate found in the central and western equatorial Pacific (Berger, Adelseck, and Mayer, 1976).

Thus, typical values of k/ω_o^2 in the Atlantic, if Lyman's constants are correct, are $2(10)^4$ ky cm^{-2} and in the Pacific are 10^4 to 10^5 ky cm^{-2}. If Mehrbach's constants are correct, k/ω_o^2 is on the order of $3(10)^6$ ky cm^{-2}.

The laboratory measured rate constant at 20°C and 1 atm pressure is $1.1(10)^7$ ky^{-1} for whole sediment and $2.1(10)^5$ ky^{-1} for the >300 μm fraction of Ontong-Java Plateau sediment (Keir, 1980).[4] Sjoberg (1978) has measured an Arrhenius activation energy of 8.4 kcal/mole for reagent grade calcite powder in seawater. If this activation energy is typical of deep-sea sediment, then at 0°C the rate constant will be one-third that at 20°C. Assuming a typical sedimentation rate, ω_o, of 2.0 to 2.5 cm/ky, the predicted value of k/ω_o^2 from the laboratory is on the order of 10^6 ky/cm^2 for whole sediment and 10^4 ky/cm^2 for the coarse fraction.

Thus if s_o is calculated using Lyman's (ms) values, it appears that the laboratory rate constant of the >300 μm fraction is comparable to the model predicted k, but the laboratory reactivity of whole sediment is two orders of magnitude greater than expected from the model. However, if Mehrbach and others' (1974) constants are employed, the laboratory reactivity of whole sediment is comparable to that predicted by the model.

It is possible that in-situ oceanic sediment exhibits lower reactivity than when the sediment is suspended in laboratory kinetics experiments. The fine fraction of settled particles may expose less surface area for dissolution as compared to when suspended. In addition, Schink and Guinasso (1978) have shown that the presence of an additional carbonate flux due to aragonite dissolution coupled with the presence of a diffusion sublayer will retard calcite dissolution. On the basis of this model, it is not possible to distinguish which scale of undersaturation is more nearly correct.

D. *Effect of a laminar boundary layer.*—Schink and Guinasso (1977) have performed a detailed analysis of the effect of a laminar boundary layer of various thicknesses on carbonate preservation utilizing linear dissolution kinetics in the pore-water. We shall very briefly consider non-linear kinetics in conjunction with a boundary-layer in this section.

The model simply assumes that a boundary layer of thickness, l, caps the sediment-water interface, and that in this layer, transport of dissolved carbonate is accomplished by molecular diffusion, where D denotes the diffusion coefficient (see fig. 5). Since no dissolved carbonate is produced

[4] Morse (1978) found similar reactivities for three other relatively undissolved sediment samples in the Atlantic, Pacific, and Indian Oceans.

in this layer, the flux, J, across the sediment-water interface and the top of the boundary layer are equal, thus,

$$J = -\phi D' M c_{eq} \frac{ds}{dx}\bigg|_{x=0+} = -D M c_{eq} \frac{ds}{dx}\bigg|_{x=0-} \tag{29}$$

where the subscripts $x = 0-$ and $x = 0+$ refer to the gradient of s in the boundary layer and below the sediment-water interface. Since the gradient in the boundary layer is linear, one obtains

$$\frac{ds}{dx}\bigg|_{x=0+} = \frac{D}{\phi D' l}(s_w - s_o) \tag{30}$$

where s_w is the undersaturation of the overlying seawater, s_o is the undersaturation at the sediment-water interface, and $(s_w - s_o)/l$ is the gradient in the boundary layer. From the definition of F,

$$F = \frac{J}{\rho(1-\phi)\omega_o}$$

and from eq (29), eq (30) becomes

$$\frac{\rho(1-\phi)\omega_o F}{\phi D' M c_{eq}} = \frac{D}{\phi D' l}(s_w - s_o) \tag{31}$$

Using values of $D' = 60$ cm^2 y^{-1}, $D = 300$ cm^2 y^{-1} and $\phi = 0.7$ one obtains

$$0.19 \frac{\omega_o F}{c_{eq}} = 7 \frac{(s_w - s_o)}{l} \tag{32}$$

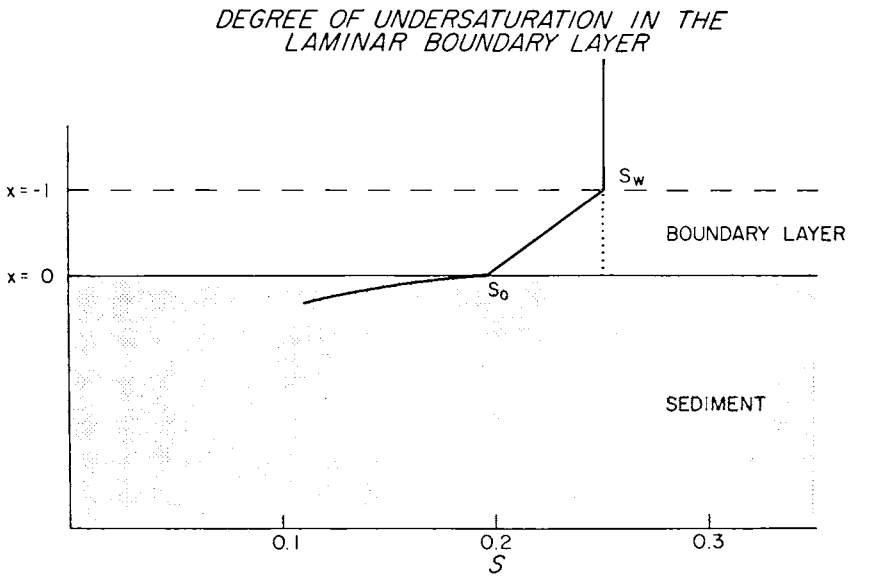

Fig. 5. Illustration of the gradient of s in presence of laminar boundary layer above sediment-water interface. In this case k = 300 y^{-1}, ω_o = 3 cm ky^{-1}, X_o = 85 percent, and l = 0.1 cm. 91 percent of the settling carbonate dissolves. Dotted line shows case of no boundary layer.

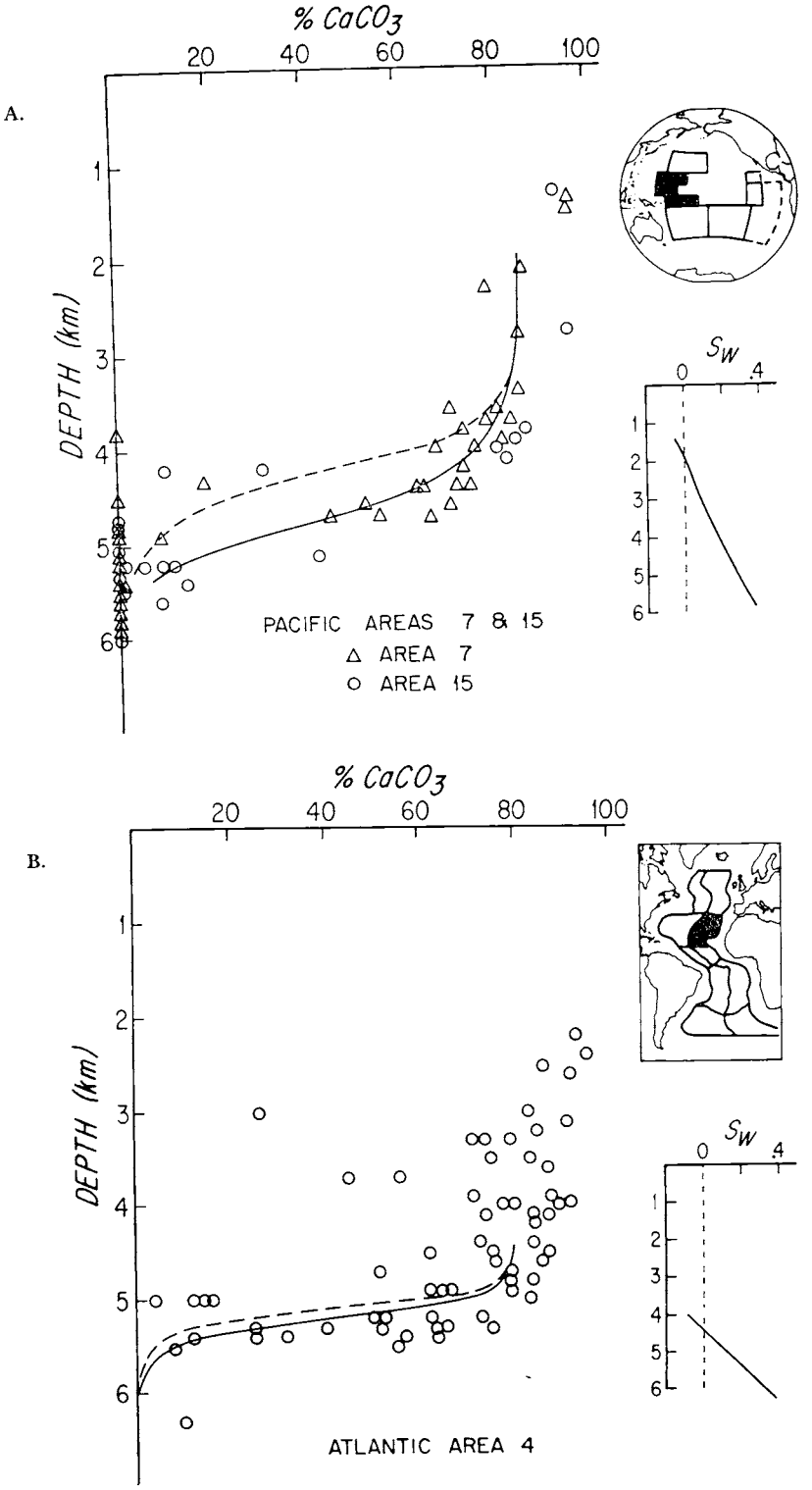
A.
% CaCO3
20
40
60
80
100
DEPTH (km)
1
2
3
4
5
6
Sw
0
.4
PACIFIC AREAS 7 & 15
△ AREA 7
○ AREA 15
B.
% CaCO3
20
40
60
80
100
DEPTH (km)
1
2
3
4
5
6
Sw
0
.4
ATLANTIC AREA 4

where c_{eq} is in mmole/l, ω_o is cm ky^{-1}, and l in cm. In eq (32), s_o and F are both unknowns. However, $s_w > s_o > 0$, and therefore one can find the correct value of s_o iteratively by using trial values, calculating F from eqs (24) and (25), and then testing for the equality given by eq (32).

We have calculated percent $CaCO_3$ versus depth in two areas, the western equatorial Pacific (7-15) and in Atlantic Area 4 using a boundary layer of 0.1 cm. In both cases, it was necessary to increase k/ω_o^2 by a factor of three to resemble the observed percent $CaCO_3$ versus depth. Figure 6 illustrates these results together with the resulting percent $CaCO_3$ versus depth curve for the same k/ω_o^2 when no boundary layer exists. It is observed that while in the equatorial Pacific, the depth of transition from high to low percent $CaCO_3$ is raised about 500 m, the transition depth in the Atlantic is altered a small amount, about 100 m. This appears to be due to the CCD corresponding to a smaller s_w in the Atlantic than in the equatorial Pacific.

6. Characteristics inherent to and predicted by the one-particle model

In the next sections, several predicted properties of the model, which are either not yet adequately observed in the field or are strictly hypothetical, are discussed.

A. *The minimum time of dissolution of a carbonate particle.*—The maximum rate of dissolution occurs at the sediment water interface. Since the rate in fraction per unit time is given by ks^n for any value of s, the minimum time of dissolution is $1/ks_o^n$. Using Lyman's constants, the value of k in many areas is about 10/yr assuming a sedimentation rate of 1 cm/ky, and the maximum value of s_o encountered at the CCD is about 0.4. With $n = 4.5$, the minimum time of dissolution of a particle is 6 yrs. If the sedimentation rate is 2.5 cm/ky, the minimum time of dissolution is about 1 yr.

Similarly, typical values for k found from the undersaturation scale proposed by Broecker and Takahashi (1978) are $3(10)^3$/yr and the typical value of s_o encountered at the CCD is 0.15. The calculated minimum time of dissolution is about 2 yrs.

B. *Particle number and size distribution as a function of s_o.*—Figure 7 illustrates the result of a calculation of β/β_o, J/J_{max} and percent $CaCO_3$ as a function of s_o when $k/\omega_o^2 = 2.1(10)^3$ ky cm^{-2} and $X_o = 90$ percent (Pacific Area 7 and 15, Lyman's constants). Figure 8 illustrates the particle size distribution and mass fraction of the calcium carbonate with progressively increasing dissolution.

Figures 7 and 8 illustrate that the particle ratio, β/β_o, (and hence the number of particles), increases at first, reaching a maximum of about 1.5 at about $s_o = 0.26$ in this example. At greater s_o, the particle ratio drops relatively rapidly. The initial increase in the number of particles per

← Fig. 6. Percent $CaCO_3$ versus depth for case of 0.1 cm thick laminar boundary layer (solid line) and in case of no boundary layer (dashed line). (A) Pacific Area 7-15, $k/\omega_o^2 = 3(10)^5$ cm^2 ky^{-1} $\omega_o = 3$ cm ky^{-1}, (B) Atlantic Area 4, $k/\omega_o^2 = 1.8(10)^5$ cm^2 ky^{-1} $\omega_o = 1.5$ cm ky^{-1}. s calculated using Lyman's (1957) constants and corrected Pacific total CO_2 data (Broecker and Takahashi, 1978).

volume is due to the fact that as one proceeds to larger undersaturations, the steady state particle size distribution shifts toward a thinner average particle size. Thus, the sediment contains more carbonate particles per volume as long as the carbonate fraction has not been strongly diluted. The maximum particle concentration occurs right on the "shoulder" of where the percent $CaCO_3$ begins to drop. At this point the time of complete dissolution of a particle is comparable to the contact time of particles in the dissolution zone. As the particle dissolution time diminishes further, the particle concentration and percent $CaCO_3$ decreases rapidly.

C. *The profile of s and dissolution rate as a function of depth in the sediment.*—Eq (28) gives the value of s as a function of depth in sediment when calcite is the only mineral dissolving. Figure 9 shows the model profiles for Pacific Area 7-15 at s_0 values of 0.1 to 0.4 (Lyman's constants). Also shown are profiles of the rate of dissolution in mg/cm³ pore water/yr. This is calculated from the expression

$$R_{(mg)} = kX_0 \frac{\beta}{\beta_0} \frac{\rho(1-\phi)}{\phi} s^n$$

As shown in figure 9, virtually all the dissolution is confined to the upper 3 or 4 mm of the sediment. It can be seen that increasing s_0 from 0 to 0.3 results in a pronounced increase in dissolution at the surface of the sediment but very little at 0.3 cm depth. Increasing the undersaturation from 0.3 to 0.4 results in a slight *decrease* in rate at the surface but slightly greater dissolution rates at all depths between 0.1 and 0.8 cm. The

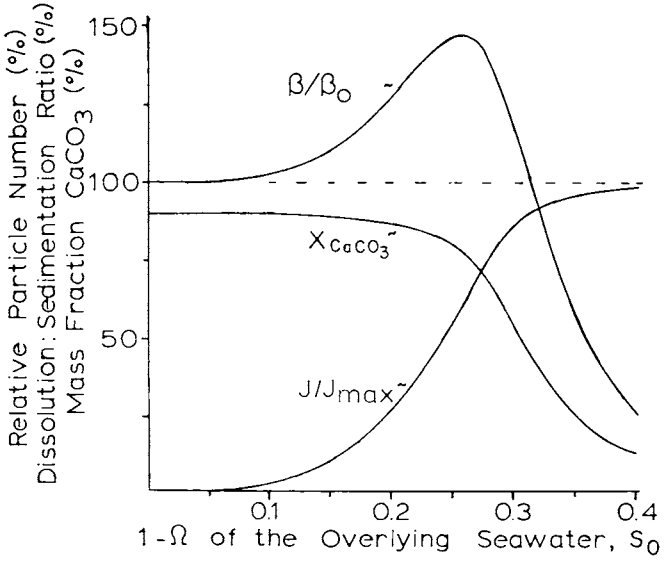

Fig. 7. Relative particle number (β/β_0), fraction of carbonate dissolved (J/J_{max}) and percent $CaCO_3$ (X_{CaCO_3}) versus s_0, $k/\omega_0^2 = 2100$ ky/cm² and initial carbonate content = 90 percent. b(z) calculated from the s_0 versus depth profile in Pacific Area 7-15.

fraction of the settling carbonate which is dissolved at $s_o = 0.3$ is 87 percent whereas at $s_o = 0.4$ it is 98 percent. Figure 7 shows that between $s_o = 0.3$ and 0.4, there is a rapid drop in particle concentration (and surface area) which is why no further increase in the dissolution rate at the sediment-water interface takes place.

Unfortunately, little information is available as to what the actual state of saturation in the interstitial water of deep-sea sediment is. Morse (1977) conducted cold-squeeze extraction of pore water from freshly obtained cores from several depths and locations in the North Atlantic. However, it is suspected that carbonate precipitated on decompression of the core. Sayles (1980) using an interstitial water sampler found the carbonate ion concentration from 1 to 10 cm below the sediment-water interface to be uniform. The carbonate ion concentrations were consistent with Ingle and others' (1973) low temperature 1 atm measurement and her measured pressure coefficient (Ingle, 1975).

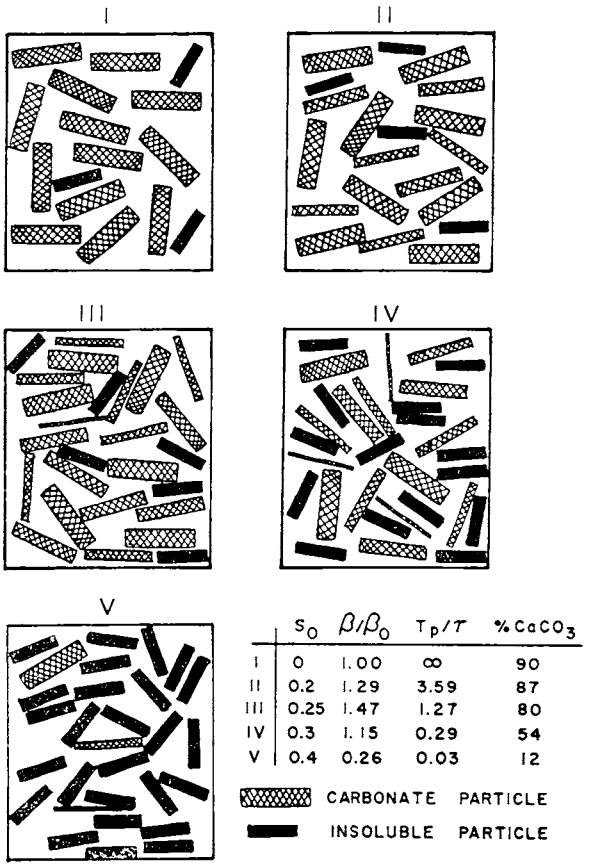

Fig. 8. Illustration of hypothetical particle distribution for the model sediment which is in various steady state stages of dissolution.

D. *The average particle thickness.*—The average particle thickness (in the case of tests, "thickness" refers to wall thickness) can be determined from the assumption that the thickness of a particle, h, diminishes at a constant rate until it vanishes at $t = t_p$. Thus

$$h(t) = h_o \left(1 - \frac{t}{t_p} \right) , \tag{33}$$

where h_o is the initial thickness of the particle, and t is the time the particle has spent in the box. The number of particles that leave the box between t and dt is

$$-\frac{d\beta^*}{dt} = \frac{\beta_o^*}{\tau} e^{-t/\tau} \tag{34}$$

where β_o^* is the number of particles added at an instant, t = 0. The

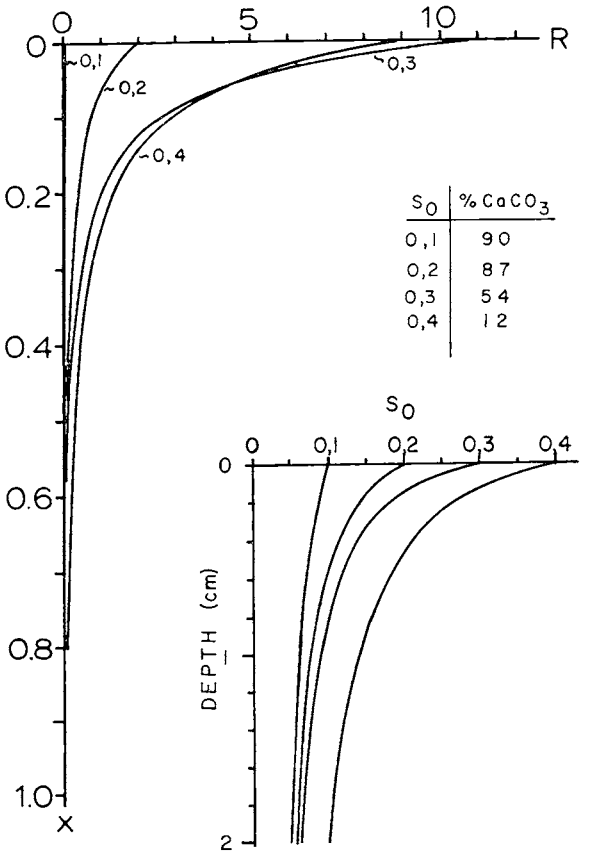

Fig. 9. Model predicted dissolution rate in mg/cm³/yr as a function of depth in sediment for the case of Pacific Area 7-15 assuming sedimentation rate of 1 cm/kyr. Value of s_o shown adjacent to curve.

average thickness is obtained by summing the number of particles multiplied by their thickness, h, and dividing by the total number of particles. Thus from (33) and (34)

$$h_{avg} = \frac{h_o \int_o^{t_p} \left(1 - \frac{t}{t_p}\right) \frac{\beta_o^*}{\tau} e^{-t/\tau}\, dt}{\int_o^{t_p} \frac{\beta_o^*}{\tau} e^{-t/\tau}\, dt}$$

$$= h_o \frac{1 - \frac{\tau}{t_p}(1 - e^{-t_p/\tau})}{1 - e^{-t_p/\tau}} \qquad (35)$$

In the case of weak dissolution $\tau << t_p$ and $h_{avs} \cong h_o$. In the case of strong dissolution, $\tau >> t_p$. In this case

$$e^{-t_p/\tau} \cong 1 - \frac{t_p}{\tau} + \frac{1}{2}\left(\frac{t_p}{\tau}\right)^2$$

Substitution of this expression in (35) yields

$$h_{avg} = \frac{h_o}{2}\left(1 - \frac{1}{2}\frac{t_p}{\tau}\right)^{-1} \cong \frac{1}{2} h_o \qquad (36)$$

Thus at high rates of dissolution the average thickness of carbonate particles is about half that of the original thickness. Therefore, the average surface area per unit mass of carbonate particle is about twice that of the undissolved particle.

The reason for this phenomenon is that at high dissolution rates where $\tau >> t_p$, the number distribution of particles that have various thicknesses in the box is very nearly uniform. That is, approximately the same number of particles that have their original thickness will exist as are those that are almost completely dissolved. This is a consequence of the assumption of perfect mixing of the solid and has certain ramifications when considering two-particle systems (see pt. B, sec. 3).

Figure 10 compares the case of $X_o = 90$ percent in figure 8 to the case of $X_o = 100$ percent calcium carbonate. In the case of 100 percent $CaCO_3$ in the sedimentation influx, dilution by insoluble material is impossible. Thus β/β_o can only increase until $\beta/\beta_o = 2$. At this point 100 percent dissolution of the influx of carbonate is occurring. Beyond $s_o = 0.29$, no real solution to eq (25) exists. The difference between dilution and no dilution with clay is also illustrated in figure 11 which shows β/β_o versus percent dissolution.

E. *Rate of dissolution as a function of $CaCO_3$ preservation.*—Previous sediment dissolution models (Schink and Guinasso, 1977; Broecker and Broecker, 1974; Emerson and Bender, 1981) have simply formulated the reactivity of sediment at a constant degree of undersaturation as proportional to the mass of reactive material in the sediment. The model formulated here, however, shows that this may not be so if the dissolution

is not first order with respect to mass. Furthermore, in a dynamic system, the dissolution may not correspond to the order or proportionality with respect to mass in a static one. In this model, the dissolution at a fixed s is presumed to be zero order with respect to a particle as long as it exists. In this case the "apparent reaction rate constant" is k β/β_0, that is, the rate is proportional to the number of particles. Thus the ratio β/β_0 is an index of relative reactive surface area of the sediment.

β/β_0 as a function of mass fraction of calcium carbonate in the sediment box is shown in figure 12. This was calculated for initial percent $CaCO_3$ of 75, 90, and 96 percent using the station data of Pacific Area 7-15. It can be seen that no simple linear relation exists. The maximum carbonate particle concentration is skewed closer to the initial percent $CaCO_3$ at higher initial values of influxing percent $CaCO_3$. The value of the maximum also increases toward the theoretical maximum of $\beta/\beta_0 = 2$ when the initial percent $CaCO_3 = 100$ percent.

F. *Effect of initial percent $CaCO_3$ upon percent dissolution versus undersaturation of the overlying water.*—In figure 13, J/J_{max} versus s_0 has

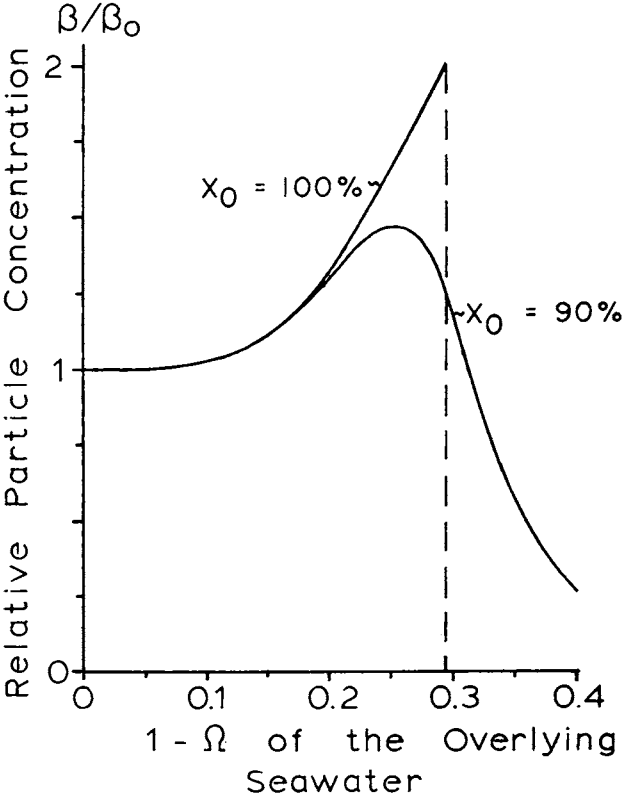

Fig. 10. Relative particle concentration versus undersaturation of the overlying water when $X_0 = 90$ and 100 percent. $k/\omega_0^2 = 2.13(10)^3$ ky/cm^2. b(z) from Pacific Area 7-15.

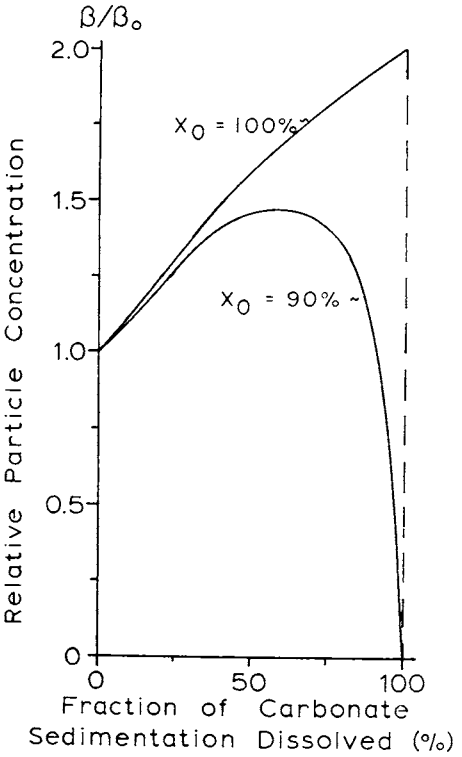

Fig. 11. Relative particle concentration versus extent of dissolution when X_o = 90 and 100 percent.

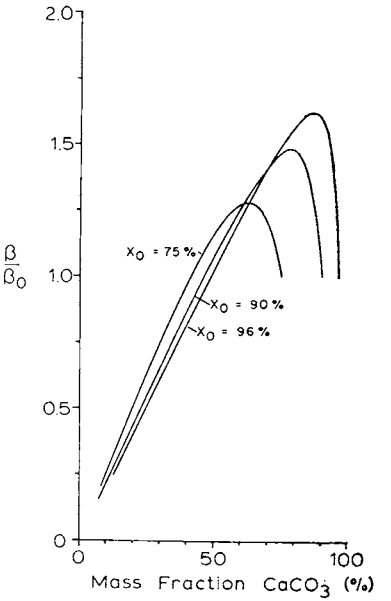

Fig. 12. Relative particle concentration versus percent $CaCO_3$ when X_o = 75, 90, and 96 percent. $k/\omega_o^2 = 2.13(10)^3$ ky/cm², and b(z) from Pacific Area 7-15.

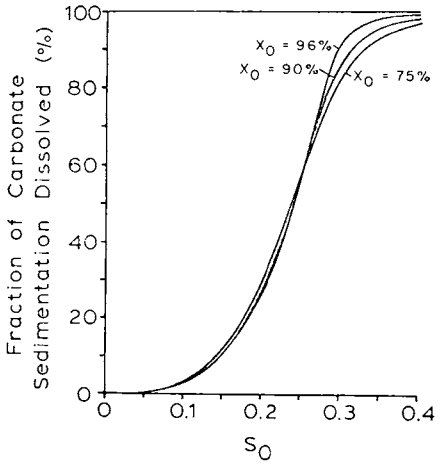

Fig. 13. Percent dissolution versus undersaturation of the overlying water when X_o = 75, 90, and 96 percent using $k/\omega_o^2 = 2.13(10)^3$ ky/cm² and b(z) at Pacific Area 7-15.

been plotted for the three initial values of percent $CaCO_3$. It can be seen that up to about 75 percent dissolution, the J/J_{max} versus depth profile is very similar. At higher J/J_{max}, the difference is less than 10 percent.

Unfortunately, J/J_{max} is still not unequivocal in the less-than-75 percent dissolution range because of uncertainties as to the correct s_o versus depth scale, as to what degree aragonite is influencing dissolution, and whether the system is truly behaving in a diffusive manner as regards the pore water. Another uncertainty is the behavior of a system where a heterogeneous mixture of various types of calcite particles are arriving at the sediment-water interface. We will examine the latter question in the following section.

B. TWO TYPES OF CALCITE PARTICLES

Besides the depth zonation in percent $CaCO_3$ in the deep sea, perhaps the best known characteristic feature of carbonate dissolution is the change in foraminiferal faunal assemblage with ocean depth, termed the foraminiferal lysocline (Berger, 1968, 1975). In this section, a modification of the basic model in part A is introduced in order to speculate upon the significance of the foram lysocline. The model will also be used to examine the effect of sedimentation of two calcite particle types with widely different reactivities.

1. Theory

We imagine the calcite influx to consist of two types of calcite particles, each with its own characteristic shape, mass, and thickness. In order to apply this model, we must postulate the mass fraction (Y) of particle one to total carbonate mass *for the undissolved influx*. Thus,

$$Y = \frac{m_1}{m_1 + m_2}$$

and

$$1 - Y = \frac{m_2}{m_1 + m_2} \tag{37}$$

where m_1 and m_2 are the total mass of type one particles and type two particles in the undissolved settling assemblage. The mass per unit particle of the undissolved particle is σ_1^0 and σ_2^0 for types 1 and 2. Thus

$$m_1 = \beta_1^0 \sigma_2^0 \text{ and } m_2 = \beta_2^0 \sigma_2^0 , \tag{37a}$$

where β_1^0 and β_2^0 are the concentrations of particles 1 and 2 in the undissolved assemblage.

The total dissolution flux out of the sediment, J, will be the sum of the dissolution flux contributions from each type of particle. Thus

$$J = J_1 + J_2 ,$$

where J_1 is contributed by type 1 and J_2 by type 2.

To solve the system for the particle concentrations, β_1 and β_2, in the sediment and the dissolution flux, we make use of three steady state

conditions. The first two state that the rate of change in the concentration of each type particle is zero, and the third is that the production of dissolved carbonate in the pore water is balanced by ionic diffusion across the sediment-water interface. As shown in the one-particle model, the particle equations are

$$\frac{\beta_i^0}{\tau_o}(1-e^{-t_i/\tau})-\frac{\beta_i}{\tau}=0 \qquad i=1,2 \tag{38}$$

where β_i^0 and β_i refer to the concentration of particles of the i^{th} type, the superscript o refers to the concentration in the case of no dissolution, t_i refers to the characteristic time it takes to dissolve each particle. It is given by the original mass per particle divided by the average rate of dissolution per particle. Thus,

$$t_i=\frac{\beta_i\sigma_i^0 L}{J_i} \qquad i=1,2 \tag{39}$$

Now we assume that the two different particles have different reaction rate constants, k_1 and k_2, and as before, the reactive surface area of each set of particles is proportional to the number of each kind of particle. Thus, the rate is proportional to f (β_1, β_2), where[5]

$$f=k_1\beta_1\sigma_1^0+k_2\beta_2\sigma_2^0 \tag{40}$$

The mass of carbonate per total sediment volume in the case of no dissolution is

$$\beta_1^0\sigma_1^0+\beta_2^0\sigma_2^0=X_o\rho(1-\phi) \tag{41}$$

From eqs (37), (37A), and (41) we obtain

$$Y=\frac{\beta_1^0\sigma_1^0}{X_o\rho(1-\phi)}$$

$$1-Y=\frac{\beta_2^0\sigma_2^0}{X_o\rho(1-\phi)} \tag{42}$$

The function f becomes (eq 40)

$$f=X_o\rho(1-\phi)\eta \tag{43}$$

where

$$\eta\equiv k_1 Y\frac{\beta_1}{\beta_1^0}+k_2(1-Y)\frac{\beta_2}{\beta_2^0}$$

If the sediment is well-stirred, the ratio β_1/β_2 is invariant with depth in sediment, thus the first term of the above definition gives the propor-

[5] $\beta_i\sigma_i^0$ is analogous to the reactive surface area, relative to undissolved sediment, multiplied by the mass of the i^{th} type carbonate per bulk volume in undissolved sediment (see eq 16B).

tion of the dissolution flux due to particle 1 dissolution, and the second term gives the proportion due to particle two. Thus

$$\frac{J_1}{J} = \frac{1}{\eta}(k_1 Y)\frac{\beta_1}{\beta_1^0}$$

$$\frac{J_2}{J} = \frac{1}{\eta}\left[k_2(1-Y)\frac{\beta_2}{\beta_2^0}\right] \tag{44}$$

Substitution of eqs (42) and (44) into (39) yields the following expression for the dissolution time of each particle type

$$t_i = \frac{X_0\rho(1-\phi)\eta L}{k_i J} \qquad i = 1,2 \tag{45}$$

Substitution into the steady state eq (38) yields

$$1 - \frac{\beta_i}{\beta_i^0}(1-F) - \exp\left[-X_0\frac{\eta}{k_i}(F^{-1}-1)\right] = 0 \qquad i = 1,2 \tag{46}$$

where F as before is the dissolution flux to *total* sedimentation flux ratio,

$$F \equiv \frac{J}{\omega_0\rho(1-\phi)}$$

This result (eq 46) is identical to the case of the one-particle model (eq 14) except that the β/β_0 term in the exponent is replaced by η/k_i.

To obtain J, we note that the rate of production of carbonate ion in the pore water at a given degree of undersaturation, s, is given by

$$R = X_0\rho\frac{(1-\phi)}{\phi}\eta s^n . \tag{47}$$

From the steady state diffusion-production equation (eq 17) we obtain

$$c_{eq}D\frac{d^2s}{dx^2} - \frac{\rho(1-\phi)}{M\phi}X_0\eta s^n = 0 \tag{48}$$

The dissolution flux is given by (eq 21)

$$J = \phi D' M c_{eq}\left(\frac{2\gamma}{n+1}S_0^{n+1}\right)^{1/2}$$

where γ is now redefined as

$$\gamma \equiv \frac{X_0\eta\rho(1-\phi)}{c_{eq}DM\phi}$$

The difference between sedimentation and accumulation rate becomes (eq 23)

$$\frac{J}{\rho(1-\phi)} = (X_0 b s_0^{n+1}\eta)^{1/2} \tag{49}$$

where b is defined as in part A, section 1 (eq 23A).

Thus the complete eqs (46) are

$$1-\frac{\beta_i}{\beta_i^0}\left[1-\frac{1}{\omega_0}(X_0 b s_0^{n+1}\eta)^{1/2}\right] - \exp\left\{-X_0\frac{\eta}{k_i}\left[\frac{\omega_0}{(X_0 b s_0^{n+1}\eta)^{1/2}}-1\right]\right\}=0$$

$$i = 1,2 \qquad (50)$$

From these functions, β_1/β_1^0 and β_2/β_2^0 are solved by a double iteration technique detailed elsewhere (Keir, ms).

The ratio of the dissolution flux to the carbonate influx is obtained from

$$\frac{J}{J_{max}} = \frac{J}{X_0\omega\rho(1-\phi)} = \frac{1}{\omega_0 X_0}(X_0 b s_0^{n+1}\eta)^{1/2} \qquad (51)$$

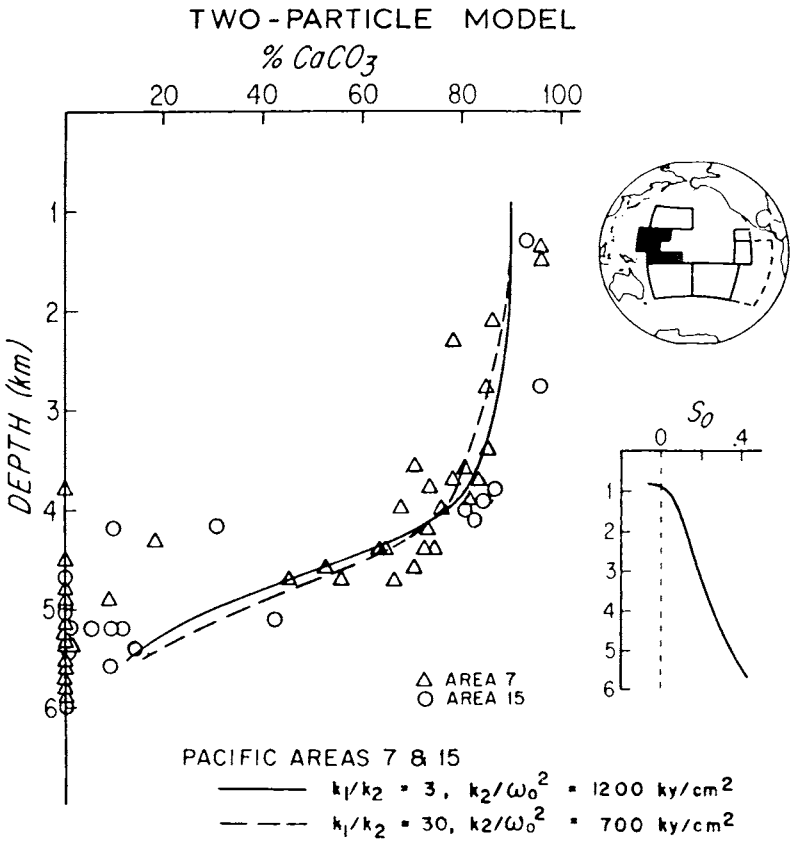

Fig. 14. Percent $CaCO_3$ versus depth in the western equatorial Pacific. Lines show approximate best fit predicted by two-particle model. Solid line — $k_1/k_2 = 3$; $k_2/\omega_0^2 = 1200$ ky/cm^2. Dotted line — $k_1/k_2 = 30$; $k_2/\omega_0^2 = 700$ ky/cm^2. Insets show area and undersaturation versus depth calculated using Lyman's (ms) K_1, K_2, and K_B and Ingle and others' (1973) calcite solubility data. Data are from Berger, Adelseck, and Meyer (1976).

2. Results and Discussion

The results of two calculated percent $CaCO_3$ versus water depth curves for Pacific Area 7-15 based on the two particle model are shown in figure 14. In both cases it has been assumed that 50 percent of the mass of carbonate influx is in the form of one particle, and 50 percent in the form of the other particle. In one calculation, it is assumed that the ratio of the reactivities (k_1/k_2) is three, in the other that it is thirty.

In the first case, it is imagined that we are dealing with two foram species, one of which has a wall three times thicker than the other. In the second case, it is imagined the system consists of particles of markedly different thicknesses such as forams and coccoliths.

As far as model calculated J/J_{max} β_1/β_1^0, β_2/β_2^0, and percent $CaCO_3$ are concerned, only the mass ratio and reactivities of the particles need to

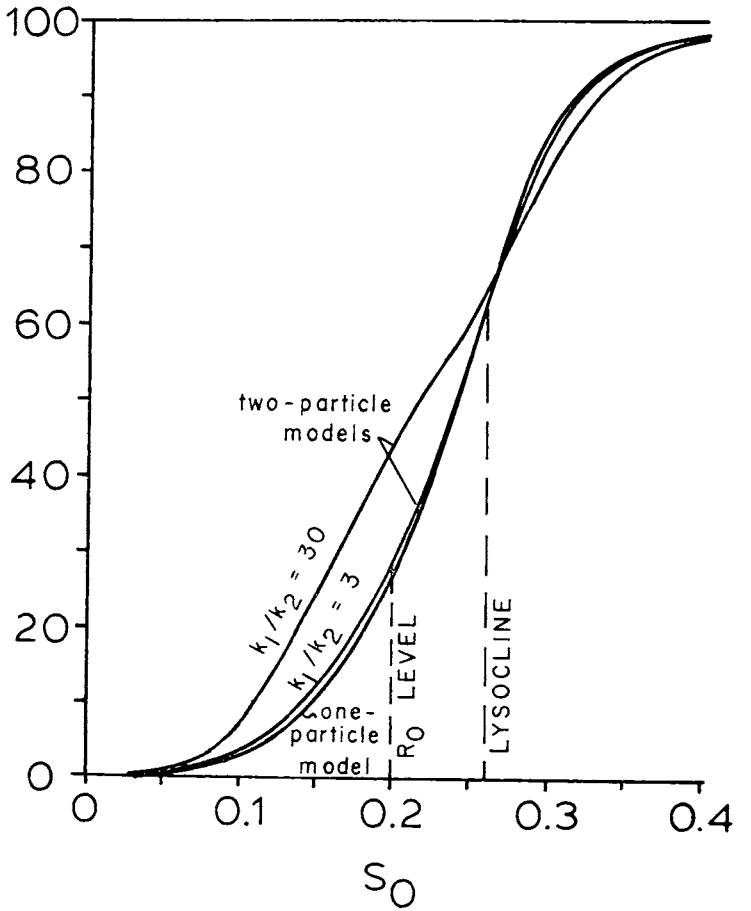

Fig. 15. Fraction of carbonate sedimentation dissolved (%) versus degree of undersaturation of overlying water for one- and two-particle models fit to percent $CaCO_3$ data in figure 14. Position of R_0 and foram lysocline estimated from figure 19.

be specified. However, if the number ratio of particle 1 to 2 as a function of dissolution is desired, the undissolved number ratio must be specified.

Figure 14 shows that with equal mass of each particle, a decent fit to the percent $CaCO_3$ versus depth curve can be found. Even if the one particle were of infinite reactivity so that it dissolved instantaneously when undersaturation at about 1 km water depth were reached, the appearance of the percent $CaCO_3$ versus depth curve would not be greatly affected because a shift from 90 to 82 percent $CaCO_3$ would be seen at about 1 km, below which an adequate curve fit to the data could be found with the appropriate reactivity of the second particle.

Figure 15 illustrates the J/J_{max} as a function of s_o for the two-particle curves and the best fit one-particle curve. It illustrates that significantly more dissolution could be taking place in the low range of s_o (less than 0.25) if very reactive particles constituting 50 percent of the sediment are present. For example, coccoliths are more reactive than forams in laboratory experiments (Keir, 1980). Whether this is true of the settled nannofossils in deep-sea sediment is not known. Certain species of coccoliths persist, albeit in poor condition, in heavily dissolved sediment with low percentage of calcium carbonate in which no foraminiferal preserva-

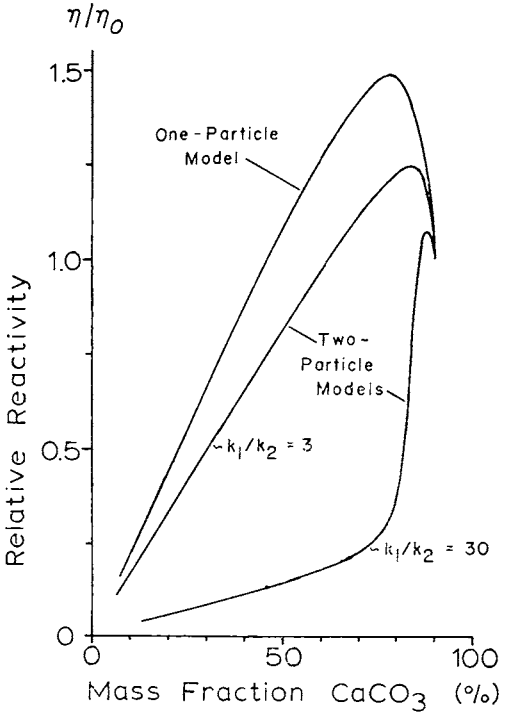

Fig. 16. Relative reactivity versus percent $CaCO_3$ for one- and two-particle models in figures 4C and 14.

tion is observed (MacIntyre and MacIntyre, 1971; Schneidermann, 1973; Honjo and Erez, 1978).

Figure 16 shows the reactive surface area relative to undissolved sediment as a function of carbonate content for the two two-particle curves and the one-particle model. This is obtained from ratio

$$\frac{\eta}{\eta_0} = \frac{\frac{k_1}{k_2}\frac{\beta_1}{\beta_1^0} + \frac{\beta_2}{\beta_2^0}}{\frac{k_1}{k_2} + 1}, \text{ when Y} = 50 \text{ percent.}$$

It is apparent that under constraint of resemblance to the observed percent $CaCO_3$ versus depth curve, the presence of a highly reactive (dissolution susceptible) particle causes the maximum in the apparent reactivity to diminish and shift closer to the initial percent $CaCO_3$ value. Also, the presence of a very reactive component causes the apparent reactivity to decrease very rapidly with decrease in percent $CaCO_3$ as the reactive component becomes severely depleted.

Figure 17 shows the ratio of β_1/β_1^0 and β_2/β_2^0 as a function of undersaturation for $k_1/k_2 = 3$ and $k_1/k_2 = 30$. The maximum in the relative particle 2 concentration versus s_o curve increases and shifts to slightly larger s_o as k_1/k_2 increases. The reverse is true for the susceptible particle.

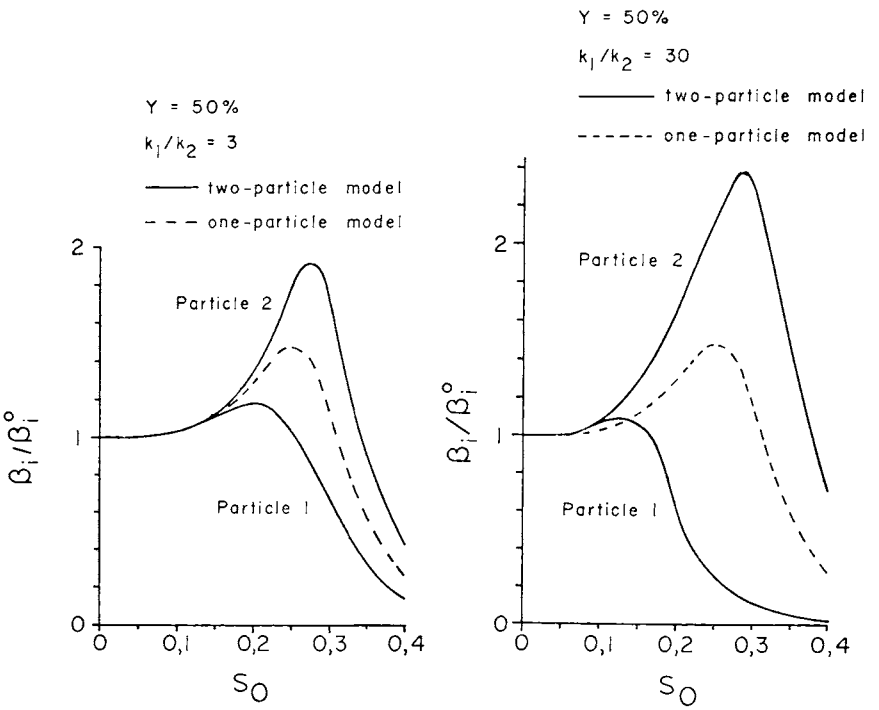

Fig. 17. Relative concentration of particle types 1 and 2 versus undersaturation of overlying water. Percent $CaCO_3$ fit to data in figure 14.

3. The Foraminiferal Lysocline

We now turn to the question of the significance of the foraminiferal lysocline. As defined by Berger (1975), the lysocline represents the depth of the inflection point in the shift from a foraminiferal species assemblage containing mostly "susceptible to dissolution" to mostly "resistant" species as water depth increases. "Susceptibility" and "resistance" are judged on the basis of whether or not a particular foram species is distinguishable from another species or not. Thus, fragmentation or severe corrosion may not altogether destroy the particle, but it may no longer be recognizable as of a particular species.

Distinction between one species assemblage and another is formulated into a "dissolution index" (Berger, 1968, 1975) where various species are ranked according to estimated susceptibility to dissolution and assigned a number, say low numbers representing high susceptibility and high numbers representing maximum resistance. On each sediment sample, various foram species with a certain size range are counted, this number is multiplied times the assigned rank, and summing through all species and dividing by the total number of forams yields the index. Thus the index is in a sense analogous to the number fraction of susceptible species to total species. But it is not exactly analogous, because the index relates to what can be recognized. With this in mind, we turn to the question of how a lysocline would appear in the simple two particle model.

The number fraction at any stage of dissolution can be found from

$$\zeta = \frac{\beta_1}{\beta_1 + \beta_2} = \frac{\dfrac{\beta_1}{\beta_1^0}\left(\dfrac{\beta_1^0}{\beta_2^0}\right)}{\dfrac{\beta_1}{\beta_1^0}\left(\dfrac{\beta_1^0}{\beta_2^0}\right) + \dfrac{\beta_2}{\beta_2^0}},$$

where β_1^0/β_2^0 is the initial ratio of number particles type 1 to particles type 2 in the influx. From the curves in figure 17, ζ as a function of s_o can be calculated if β_1^0/β_2^0 is known. For an initial value of $\beta_1^0/\beta_2^0 = 8$, $\zeta_o = 0.89$. Figure 18 shows the variation of ζ as a function of s_o for the two calculated models. A sigmoidal curve with inflection at about $s_o = 0.25$ is observed in both cases. As the reactivity ratios of the particles are increased, the magnitude of the change in number fraction is increased. As 100 percent dissolution is approached, ζ appears to approach a constant value in both cases.

We shall now proceed to compare the change in number fraction, ζ, to the change in the "dissolution index" of Berger. Berger (1975) plotted a foraminiferal "dissolution index" (FDX) versus depth for central and western equatorial Pacific sediment as a function of water depth. This is shown in figure 19. The sediment index numbers had a range from about 3.7 to 10 in this particular index scale with the low number representing high susceptibility. It is important to note that the most highly resistant species had an effective rank of 10. Apparently, none of the foraminifera less resistant than the number 10 category are found below the foram

lysocline, and the number ratio of susceptible to resistant forms shifts to zero.

Turning back to the model, from figure 18 we see that the magnitude of the change in number ratio increases as the ratio k_1/k_2 increases. In laboratory dissolution experiments, the rate of dissolution in percent/day appears to be roughly correlated to wall thickness (Adelseck, 1978; Keir, 1980). Because the resistant species have wall thicknesses 3 to 5 times the susceptible, we can expect k_1/k_2 ratios between susceptible to resistant species to be on that order. Thus, as seen particularly in the case of $k_1/k_2 = 3$, the model fails to predict correctly the observation that the number ratio, ζ, should go to zero.

This failure is due to the assumption that all particles in the zone of dissolution are well-mixed. In such a system, the number distribution of particles that are in various stages of partial dissolution approaches uniformity when the time of dissolution of a particle becomes much shorter than the time it takes to dissolve the particle. That is, at high dissolution stages, the number of particles that are almost completely dissolved equals the number that have not yet undergone any dissolution in a well-mixed system. Thus, it is expected there will always exist some

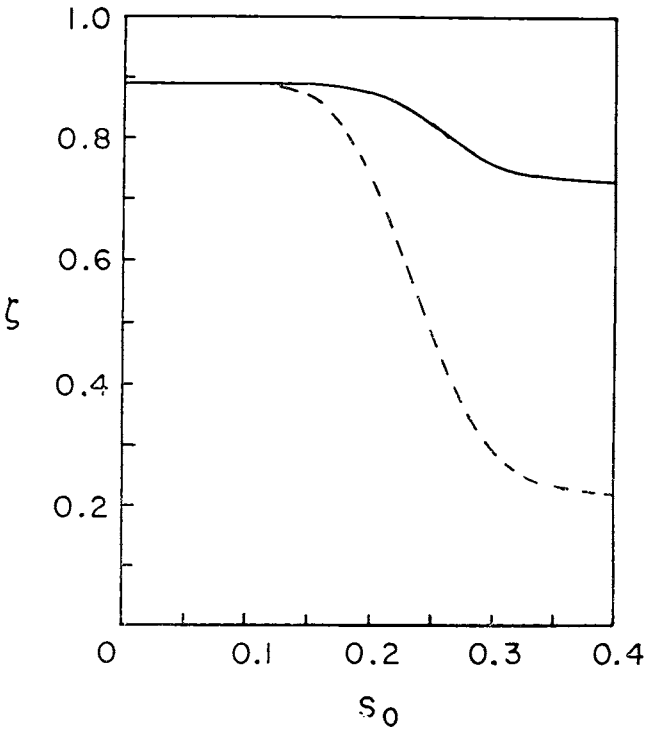

Fig. 18. Number fraction of particle 1 versus undersaturation of the overlying water. Solid line — $k_1/k_2 = 3$; dashed line — $k_1/k_2 = 30$.

relatively undissolved susceptible forams in the sediment, and *the failure to find such implies that the dissolution time of these susceptible forams below the lysocline is less than the time scale of sediment mixing.*

As shown in part A, section 1, if the zone of dissolution is confined to the upper 3 mm of sediment, the mixing time can be estimated from the Pb^{210} tracer distribution to be about half a year. Assuming that the sediment is *not* mixed well on the time scale of dissolution, a minimum estimate can be made of the rate constant based on the mixing time and the degree of undersaturation at the depth of complete foraminiferal destruction. This constant can be compared to the rate constant obtained by trial and error correspondence between the model curve and the observed percent $CaCO_3$ versus depth data.

In the case of the s_o versus depth curve derived from Lyman's constants and "uncorrected" Pacific ΣCO_2 data, the s_o value at the base of the "lysocline" is about 0.4. The minimum value of k_f for the forams can be estimated from $1/k_f s_o^n < 1/2$ yr, or $k_f > 124\ y^{-1} \sim 10^5\ ky^{-1} \sim 30$ percent/day. The measured laboratory rate constants of forams in seawater at 1 atm 20°C are about 70 percent/day (Keir, 1980), which is in good agreement with the above estimate.

However, from figure 14 we see that k_2/ω_o^2 of the *less* reactive carbonate must be on the order of 10^3 ky/cm^2 in order to predict correctly the observed percent $CaCO_3$ versus depth. Assuming a sedimentation rate

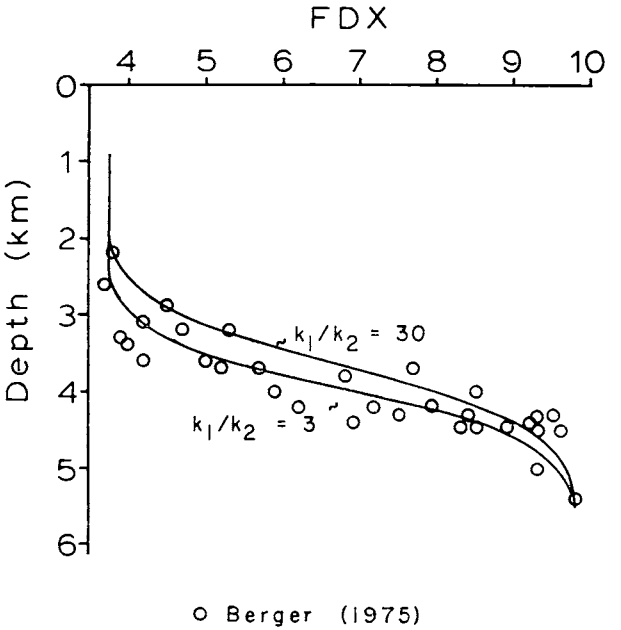

Fig. 19. Foraminiferal dissolution index versus depth. Solid lines show predicted curves from model based on the *ad hoc* procedure given in text. Circles show data from Berger (1975).

of 3 cm/ky, the reactivity of the less reactive fraction is about 10 y^{-1}, which is an order of magnitude lower than that expected of susceptible forams. *Thus, if Lyman's constants are correct, the forams are more reactive than other carbonate sediment components.*

In the case where s_o versus depth is derived according to Broecker and Takahashi (1978), the value of s_o at the base of the lysocline is about 0.25. If forams are dissolving on a time scale shorter than 1/2 yr $k_f > 10^3$ y^{-1}, which is a factor of five larger than laboratory measured rates. From figure 5 and table 1, we see that the k_2/ω_o^2 value for the less reactive sediment component is on the order of 10^5 ky/cm^2. Again, if $\omega_o = 3$ cm/ky, $k_2 \sim 10^3$ y^{-1}. *If the Broecker and Takahashi (1978) scale is correct, the forams have a reactivity equal to or greater than the other carbonate sediment components.*

Both cases are opposite of what is expected from laboratory measurements on suspended sediment, where the fine component dissolves more rapidly than the coarse (Morse, 1978; Keir, 1980). The mechanism for the inferred preferential preservation of the fine fraction is not known.

In order to estimate the amount of dissolution occurring at the lysocline in the equatorial Pacific, the model predicted number fraction change will be "normalized" to the shift in FDX. For the two-particle model, we assign the rank of 3.75 to the susceptible particle (no. 1) and 9.8 to particle 2. We shall assume that at $s_o = 0.4$, particle one is no longer recognizable due to corrosion and mechanical breakage. This abandons the postulation of the particle-ones being well-stirred on a time scale short compared to dissolution at depths below the lysocline. This is equivalent to postulating that in the case of $k_1/k_2 = 3$, particle one is not recognizable as particle one when about 15 percent of the number of particle one remains, and that in the case of $k_1/k_2 = 30$, particle one is not recognizable when about 2 percent of its number remain (see fig. 17). On the other hand particle two is postulated always to be recognizable when it is in the sediment. With this in mind, it follows that when no dissolution occurs, $\zeta_o = 0.89$ is equivalent to $FDX_o = 3.75$ and when dissolution approaches 100 percent, ζ_{100} taken as the value of ζ at $s_o = 0.4$, is equivalent to $FDX_{100} = 9.8$. Assuming a linear relationship between ζ and FDX one obtains

$$FDX = m(\zeta - \zeta_o) + FDX_o \tag{52}$$

where

$$m \equiv \frac{FDX_{100} - FDX_o}{\zeta_{100} - \zeta_o}$$

In figure 19, Berger's plot of observed FDX versus water depth values are shown. Also shown are the curves of FDX calculated from the model results according to the *ad hoc* normalization. The agreement in the case of $k_1/k_2 = 3$ is good; in the case of $k_1/k_2 = 30$, the model curve is a little high. Increasing reactivity of one particle relative to another tends to cause the lysocline to shift to a shallower depth, but this effect is not particularly sensitive to k_1/k_2 changes.

The question occurs as to how much dissolution is occurring at various depths associated with features of the index. If the lysocline is defined as the inflection point of the index (Berger, 1975), we see that it occurs at about 4 km depth in both the observed data and in the model in the case of $k_1/k_2 = 3$. This depth corresponds to $s_o = 0.26$ (when Lyman's constants are employed), and this corresponds to 63 percent dissolution in figure 15. If the transitional part of the curve is extrapolated to FDX_o, we obtain what is referred to by Berger as the R_o level, in this case located at about 3.2 km depth. This depth corresponds to $s_o = 0.2$ which from figure 15 yields 29 percent dissolution. This compares reasonably well to Adelseck's (1978) estimate that 80 percent *of the forams* at the lysocline and 50 percent *of the forams* at the R_o level were destroyed. However, a cautionary note on these estimates is the observation that the presence of aragonite dissolution in the sediment reduces the dissolution rates corresponding to lower s_o values. For example, the one-particle calcite dissolution model (Keir, ms) with aragonite dissolution in the top 2 mm of sediment yields $J/J_{max} = 53$ percent at $s_o = 0.26$ and $J/J_{max} = 10$ percent at $s_o = 0.2$. Thus, despite the fact that Adelseck's (1978) experiments indicate a significant foram dissolution before recognition of facies change, aragonite might be inhibiting such dissolution until a sudden increase in the dissolution takes place (Schink and Guinasso, 1978).

SUMMARY

The considerations taken into account in the one- and two-type carbonate models suggest the following:

1. The percent $CaCO_3$ versus depth patterns in the Atlantic and Pacific can be explained reasonably well on the basis of the interaction of the carbonate dissolution kinetics, the undersaturation of the overlying water, ionic diffusion, and bioturbation.

2. If dissolution is forced solely by the undersaturation of the overlying water, most dissolution takes place in the upper 3 mm of the sediment.

3. The reactive surface area of the calcite may not correlate linearly with the percent $CaCO_3$.

4. It appears that boundary layer effects upon preservational horizons are more pronounced at greater degree of undersaturation, such as in the equatorial Pacific.

5. Susceptible forams in sediment below the lysocline dissolve at rates that are less than the time it takes to mix them throughout the depth zone of dissolution in sediment. This conclusion agrees with laboratory rates but is larger than expected on the basis of the percent $CaCO_3$ versus depth curve.

6. Provisionally, it appears that 10 to 30 percent of the settling calcite dissolves at the R_o level in the equatorial Pacific, and 50 to 65 percent dissolves at the inflection of the FDX, termed the foram lysocline by Berger (1975).

7. If a reactive component is present in the initial settling assemblage, it can contribute an "unseen" dissolution flux at relatively low undersaturations.

ACKNOWLEDGMENTS

The work presented here was originally begun at the late stages of the author's Ph.D. research. The work expanded almost uncontrollably as divergent opinions arose, first from my thesis committee and then from journal reviewers, concerning suggested improvements and faults in the manuscript. In the interim, the GEOSECS data base was also continuously being reviewed. As a consequence, much of the work has been recalculated, revised, and expanded at the Woods Hole Oceanographic Institution.

I would like to thank R. A. Berner for his support and many suggestions. B. Boudreau, P. Brewer, M. Fiadeiro, R. Hall, A. Lasaga, T. Takahashi, and K. K. Turekian have all provided constructive reviews and criticism. K. K. T. kindly provided use of his minicomputer for the original calculations (after we discovered how to do this symbiotically with his gamma spectrum counting demands on the instrument). S. Honjo kindly provided support for the subsequent work at W.H.O.I.

I thank the GEOSECS executive committee for permission to use the titration alkalinity and total CO_2 data, which exist largerly due to the efforts of the late Arnold Bainbridge, and particularly thank T. Takahashi and P. Brewer for their assistance in providing the most refined data set available. I thank S. Pelletier for her infinite patience in typing the paper.

Financial support was provided at various stages through NSF grants OCE73-60365, GA40002, OCE77-03473, OCE77-27080, and OCE-79-09456.

REFERENCES

Adelseck, C. G., 1978, Dissolution on deep-sea carbonate: preliminary calibration of preservational and morphologic aspects: Deep-Sea Research, v. 25, p. 1167-1185.

Adelseck, C. G., and Berger, W. H., 1975, On the dissolution of planktonic foraminifera and associated microfossils during settling and on the sea floor, *in* Sliter, W., Be, A. W. H., and Berger, W., eds., Dissolution of Deep-Sea Carbonates: Cushman Foundation for Foraminiferal Research, Spec. Pub. 13, p. 70-81.

Arrhenius, G., 1952, Sediment cores from the East Pacific: Swedish Deep-Sea Exped. (1947-1948) Repts., v. 5, n. 1-4, p. 1-228.

Berger, W. H., 1968, Planktonic foraminifera: selective solution and paleoclimatic interpretation: Deep-Sea Research, v. 15, p. 31-43.

———— 1973, Deep-sea carbonates: Pleistocene dissolution cycles: Jour. Foram. Research, v. 3, p. 187-195.

———— 1975, Deep-sea carbonates: dissolution profiles from foraminiferal preservation, *in* Sliter, W., Be, A. W. H., and Berger, W., eds., Dissolution of Deep-Sea Carbonates: Cushman Foundation for Foraminiferal Research, Spec. Pub. 13, p. 82-86.

———— 1977, Glacial-Holocene transition in deep-sea carbonates: selective dissolution and the stable isotope signal: Science, v. 197, p. 536-566.

Berger, W. H., Adelseck, C. G., and Mayer, L. A., 1976, Distribution of carbonate in surface sediments of the Pacific Ocean: Jour. Geophys. Research, v. 81, p. 2617-2627.

Berger, W. H., and Piper, D. J. W., 1972, Planktonic foraminifera: differential settling, dissolution and redeposition: Limnology Oceanography, v. 17, p. 275-287.

Berner, R. A., 1976, The solubility of calcite and aragonite in seawater at atmospheric pressure and 34.5‰ salinity: Am. Jour. Sci., v. 276, p. 713-730.

———— 1977, Sedimentation and dissolution of pteropods in the ocean, *in* Andersen, N. R., and Malahoff, A., eds., The Fate of Fossil Fuel CO_2 in the Oceans: New York, Plenum Press, p. 243-260.

Biscaye, P. E., Kolla, V., and Turekian, K. K., 1976, Distribution of calcium carbonate in surface sediments of the Atlantic Ocean: Jour. Geophys. Research, v. 81, p. 2595-2603.

Broecker, W. S., 1971, Calcite accumulation rates and glacial to interglacial changes in oceanic mixing, *in* Turekian, K. K., ed., Late Cenozoic Ages: New Haven, Yale Univ. Press, p. 239-265.

———— 1974, Chemical Oceanography: New York, Harcourt Brace Jovanovich, 214 p.

Broecker, W. S., and Broecker, S., 1974, Carbonate dissolution on the flank of the East Pacific Rise: Soc. Econ. Paleontologists Mineralogists Spec. Pub., v. 20, p. 44-57.

Broecker, W. S., and Takahashi, T., 1977, Neutralization of fossil fuel CO_2 by marine carbonate, *in* Andersen, N. R., and Malahoff, A., eds., The Fate of Fossil Fuel CO_2 in the Oceans: New York, Plenum Press, p. 243-260.

———— 1978, The relationship between lysocline depth and *in-situ* carbonate ion concentration: Deep-Sea Research, v. 26, p. 65-95.

Culberson, C. H., ms, 1972, Processes affecting the oceanic distribution of carbon dioxide: Ph.D. dissert., Oregon State Univ., 178 p.

Culberson, C., and Pytowicz, R. M., 1968, Effect of pressure on carbonic acid, boric acid and the pH in sea water: Limnology Oceanography, v. 13, p. 403-417.

Denbigh, K. G., 1944, Velocity and yield in continuous reaction systems: Faraday Soc. Trans., v. 40, p. 352-373.

Edmond, J. M., 1974, On the dissolution of carbonate and silicate in the deep ocean: Deep-Sea Research, v. 21, p. 455-480.

Edmond, J. M., and Gieskes, J., 1970, On the calculation of the degree of saturation of sea water with respect to *in-situ* conditions: Geochim. et Cosmochim. Acta, v. 34, p. 1261-1291.

Emerson, S., and Bender, M., 1981, Carbon fluxes at the sediment-water interface of the deep-sea: calcium carbonate preservation: Jour. Marine Research, v. 39, p. 139-162.

Gardner, J. V., 1975, Late Pleistocene carbonate dissolution cycles in the eastern Equatorial Atlantic: Cushman Foundation for Foraminiferal Research, Spec. Pub. 13, p. 129-141.

Hindman, J. C., ms, 1943, Properties of the system $CaCO_3$–CO_2–H_2O in sea water and NaCl solutions: Ph.D. dissert., Univ. California, Los Angeles, 160 p.

Honjo, S., 1975, Dissolution of suspended coccoliths in the deep-sea water column and sedimentation of coccolith ooze, *in* Sliter, W., Be, A. W. H., and Berger, W., eds., Dissolution of Deep-Sea Carbonates: Cushman Foundation for Foraminiferal Research, Spec. Pub. 13, p. 70-81.

———— 1977, Biogenic carbonate particles in the oceans; do they dissolve in the water column?, *in* Andersen, N., and Malahoff, A., eds., The Fate of Fossil Fuel CO_2 in the Oceans: New York, Plenum Press, p. 269-294.

Honjo, S., and Erez, J., 1978, Dissolution rates of calcium carbonates in the deep ocean; an in-situ experiment in the North Atlantic Ocean: Earth Planetary Sci. Letters, v. 40, p. 287-300.

Ingle, S. E., 1975, Solubility of calcite in the ocean: Marine Chemistry, v. 3, p. 301-319.

Ingle, S. E., Culberson, C. H., Hawley, J. B., and Pytkowicz, R. M., 1973, The solubility of calcite in sea water at atmospheric pressure and 35‰ salinity: Marine Chemistry, v. 1, p. 295-307.

Johnson, T. C., Hamilton, E. L., and Berger, W. H., 1977, Physical properties of calcareous ooze; control by dissolution at depth: Marine Geology, v. 24, p. 259-277.

Keir, R. S., ms, 1979, The dissolution kinetics of biogenic calcium carbonate in seawater: laboratory measurement and geochemical implications: Ph.D. dissert., Yale Univ., 284 p.

———— 1979, The calculation of carbonate ion concentration from total CO_2 and titration alkalinity: Marine Chemistry, v. 8, p. 95-98.

———— 1980, The dissolution of biogenic calcium carbonate in seawater: Geochem. et Cosmochim. Acta, v. 44, p. 241-252.

Kolla, V. R., Be, A. W. H., and Biscaye, P. E., 1976, Calcium carbonate distribution in surface sediments of the Indian Ocean: Jour. Geophys. Research, v. 81, p. 2605-2616.

Li, Y.-H., and Gregory, S., 1974, Diffusion of ions in seawater and in deep-sea sediments: Geochim. et Cosmochim. Acta, v. 38, p. 703-714.

Luz, B., and Shackleton, N. J., 1975, $CaCO_3$ solution during the past 130,000 years: Cushman Foundation for Foraminiferal Research, Spec. Pub. 13, p. 142-150.

Lyman, J., ms, 1956, Buffer mechanism of seawater: Ph.D. dissert., Univ. California at Los Angeles, 196 p.

MacIntyre, A., and MacIntyre, R., 1971, Coccolith concentrations and differential solution in oceanic sediments, *in* Funnell, B. M., and Riedel, W. R., eds., The Micropaleontology of Oceans: London, Cambridge Univ. Press, p. 253-261.

Mehrbach, C., Culberson, C. H., Hawley, J. E., and Pytkowicz, R. M., 1974, Measurement of the apparent dissociation constants of carbonic acid in seawater at atmospheric pressure: Limnology Oceanography, v. 18, p. 897-907.

Morse, J. W., 1977, The carbonate chemistry of North Atlantic Ocean deep-sea sediment pore water, *in* Andersen, N. and Malahoff, A., eds., The Fate of Fossil Fuel CO_2 in the Oceans: New York, Plenum Press, p. 269-294.

———— 1978, Dissolution kinetics of calcium carbonate in seawater. VI. The near-equilibrium dissolution kinetics of calcium carbonate-rich sea sediments: Am. Jour. Sci., v. 278, p. 344-353.

Morse, J. W., and Berner, R. A., 1972, Dissolution kinetics of calcium carbonate in sea water. II. A kinetic origin for the lysocline: Am. Jour. Sci., v. 272, p. 840-851.

Nozaki, Y., Cochran, J. K., Turekian, K. K., and Keller, G., 1977, Radiocarbon and Pb^{210} distribution in submersible taken deep-sea cores from Project FAMOUS: Earth Planetary Sci. Letters, v. 34, p. 167-173.

Peng, T., Broecker, W. S., and Berger, W. H., 1979, Rates of benthic mixing in deep-sea sediment as determined by radioactive tracers: Quaternary Research, v. 11, p. 141-149.

Pytkowicz, R. M., and Fowler, G. A., 1967, Solubility of foraminifera in sea water at high pressures: Geochem. Jour., v. 1, p. 169-182.

Roth, P. H., and Berger, W. H., 1975, Distribution and dissolution of coccoliths in the South and Central Pacific, *in* Sliter, W., Be, A. W. H., and Berger, W., eds., Dissolution of Deep Sea Carbonates: Cushman Foundation for Foraminiferal Research, Spec. Pub. 13, p. 87-113.

Sayles, F. L., 1980, The solubility of $CaCO_3$ in seawater at 2°C based upon in-situ sampled pore water composition: Marine Chemistry, v. 9, p. 223-235.

Schink, D. R., and Guinasso, N. L., 1977, Modeling the influence and bioturbation and other processes on calcium carbonate dissolution at the sea floor, *in* Andersen, N. and Malahoff, A., eds., The Fate of Fossil Fuel CO_2 in the Oceans: New York, Plenum Press, p. 375-399.

Schink, D. R., and Guinasso, N. L., 1978, Possible role of aragonite in separating the calcite lysocline from the depth of calcite saturation: EOS, v. 59, p. 411.

Schneidermann, N., 1973, Deposition of coccoliths in the compensation zone of the Atlantic Ocean, *in* Smith, L. A., and Hardenbol, J., eds., Proceeding of the Symposium on Calcareous Nannofossils: Soc. Econ. Paleontologist and Mineralogists, Gulf Coast Sec., p. 140-151.

Sjöberg, E. L., 1978, Kinetics and mechanism of calcite dissolution in aqueous solutions at low temperatures: Stockholm Contr. in Geology, v. 32, p. 1-92.

Takahashi, T., 1975, Carbonate chemistry of sea water and the calcite compensation depth in the oceans: Cushman Foundation for Foraminiferal Research, Spec. Pub. 13, p. 11-26.

Takahashi, T., Kaiteris, P., Broecker, W. S., and Bainbridge, A. E., 1976, An evaluation of the apparent dissociation constants of carbonic acid in seawater: Earth Planetary Sci. Letters, v. 32, p. 458-467.

Takahashi, T., and Broecker, W. S., 1977, Mechanisms for calcite dissolution on the sea floor, *in* Andersen, N., and Malahoff, A., eds., The Fate of Fossil Fuel CO_2 in the Oceans: New York, Plenum Press, p. 455-477.